Biogeosciences Discuss., https://doi.org/10.5194/bg-2018-430
Manuscript under review for journal Biogeosciences
Discussion started: 17 October 2018

Biogeosciences Discussions Open Access EGU

Unifying soil organic matter formation and persistence frameworks: the MEMS model

Andy D. Robertson*[1,2], Keith Paustian[1,2], Stephen Ogle[2,3], Matthew D. Wallenstein[1,2], Emanuele Lugato[4], M. Francesca Cotrufo[1,2]

[1] Department of Soil and Crop Sciences Colorado State University, Fort Collins, CO 80523, USA
[2] Natural Resources Ecology Laboratory, Colorado State University, Fort Collins, CO 80523, USA
[3] Department of Ecosystem Science and Sustainability, Colorado State University, Fort Collins, CO 80523, USA
[4] European Commission, Joint Research Centre, Directorate for Sustainable Resources, Via E. Fermi 2749, I-21027, Ispra (VA), Italy

Correspondence to: Andy D. Robertson (Andy.Robertson@colostate.edu)

Abstract. Soil organic matter (SOM) dynamics in ecosystem-scale biogeochemical models have traditionally been simulated as immeasurable fluxes between conceptually-defined pools. This greatly limits how empirical data can be used to improve model performance and reduce the uncertainty associated with their predictions of carbon (C) cycling. Recent advances in our understanding of the biogeochemical processes that govern SOM formation and persistence demand a new mathematical model with a structure built around key mechanisms and biogeochemically-relevant pools. Here, we present one approach that aims to address this need. Our new model (MEMS v1.0) is developed upon the Microbial Efficiency-Matrix Stabilization framework which emphasises the importance of linking the chemistry of organic matter inputs with efficiency of microbial processing, and ultimately with the soil mineral matrix, when studying SOM formation and stabilization. Building on this framework, MEMS v1.0 is also capable of simulating the concept of C-saturation and represents decomposition processes and mechanisms of physico-chemical stabilization to define SOM formation into four primary fractions. After describing the model in detail, we optimise four key parameters identified through a variance-based sensitivity analysis. Optimisation employed soil fractionation data from 154 sites with diverse environmental conditions, directly equating mineral-associated organic matter and particulate organic matter fractions with corresponding model pools. Finally, model performance was evaluated using total topsoil (0-20 cm) C data from 8192 forest and grassland sites across Europe. Despite the relative simplicity of the model, it was able to accurately capture general trends in soil C stocks across extensive gradients of temperature, precipitation, annual C inputs and soil texture. The novel approach that MEMS v1.0 takes to simulate SOM dynamics has the potential to improve our forecasts of how soils respond to management and environmental perturbation. Ensuring these forecasts are accurate is key to effectively informing policy that can address the sustainability of ecosystem services and help mitigate climate change.

1 Introduction

The biogeochemical processes that govern soil organic matter (SOM) formation and persistence impact more than half of the terrestrial carbon (C) cycle, and thus play a key role in climate–C feedbacks (Jones and Falloon, 2009; Arora *et al*., 2013). In order to predict changes to the C cycle, it is imperative that mathematical models describe these processes accurately. However, most ecosystem-scale biogeochemical models represent SOM dynamics with first-order transfers between conceptual pools defined by turnover time, limiting their capacity to incorporate recent advances in scientific understanding of SOM dynamics (Campbell and Paustian, 2015). Due to the use of conceptual

pools, empirical data from SOM fractionation cannot be used directly to constrain parameter values that govern fluxes between pools because diverse SOM compounds can have similar turnover times but are differentially influenced by environmental variables (Schmidt *et al*., 2011; Lehmann and Kleber, 2015). As a result, empirical data is commonly abstracted and transformed before being used to parameterize or evaluate the processes of SOM formation and persistence that the model is intended to simulate (Elliott *et al*., 1996; Zimmermann *et al*., 2007). This has resulted in many conventional SOM models (e.g., RothC, [Jenkinson and Rayner, 1977], DNDC [Li *et al*., 1992], EPIC [Williams *et al*., 1984] and CENTURY [Parton *et al*., 1987]) being structurally similar (i.e., partitioning total SOM into discrete pools based on turnover times determined from radiocarbon experiments; see Stout and O'Brien [1973] and Jenkinson [1977]) but each taking different approaches to simplify the complex mechanisms that govern SOM dynamics. Consequently, simulations of SOM can vary greatly between models, often predicting contrasting responses to the same driving inputs and environmental change (e.g., Smith *et al*., 1997).

Structuring SOM models around functionally-defined and measurable pools that result from known biogeochemical processes is one way to help minimise these discrepancies. Two recent insights into SOM dynamics present a path towards addressing this issue. There is now strong evidence that: 1) low molecular weight, chemically labile molecules, primarily of microbial origin (Liang *et al*., 2017), persist longer than chemically recalcitrant C structures when protected by organo-mineral complexation (Mikutta *et al*., 2006; Kögel-Knabner *et al*., 2008; Kleber *et al*., 2011); and 2) each soil type has a finite limit to which it can accrue C in mineral-associated fractions (i.e., the C-saturation hypothesis) (Six *et al*., 2002; Stewart *et al*., 2007; Gulde *et al*., 2008; Ahrens *et al*., 2015). Structuring a SOM model around these known and quantifiable biogeochemical pools and processes has the potential to drastically reduce uncertainty by enhancing opportunities for parameterization and validation of models with empirical data.

Conventional SOM models readily acknowledge the importance of microbes in plant litter decomposition and SOM dynamics but model improvement was initially constrained by the concept that stable SOM included 'humified' compounds (Paul and van Veen, 1978). This quantified stable SOM using an operational proxy (high pH alkaline extraction) rather than relating stabilization to the mechanisms that are now widely recognised, such as organo-mineral interactions and aggregate formation (Lehmann and Kleber, 2015). As our contemporary understanding of stable SOM moves away from humification theory, so too must the way we represent SOM stabilization pathways in biogeochemical models. Similarly, many SOM models partition plant residues into labile and recalcitrant pools with turnover times that reflect the assumption of 'selective preservation' (i.e., chemically recalcitrant litter-C is only used by microorganisms when labile compounds are scarce). While many existing models do include a flux from labile residues into stable SOM, this is typically a much smaller absolute amount than the flux from recalcitrant residues. Evidence indicates that biochemically recalcitrant structural litter C compounds may not be as important in the formation of long-term persistent SOM as originally thought (Marschner *et al*., 2008; Dungait *et al*., 2012; Kallenbach *et al*., 2016). Instead, they form light particulate organic matter (POM) (Haddix *et al*., 2015), a relatively vulnerable fraction of SOM with a turnover time of years to decades (von Lützow *et al*., 2006; 2007). Consequently, there have been several calls to represent this new understanding and re-examine how microbial activity is simulated in SOM models (Schmidt *et al*., 2011; Moorhead *et al*., 2014; Campbell and Paustian, 2015).

Current conceptual frameworks more clearly link the role of microbes to SOM dynamics (e.g., Cotrufo *et al*., 2013 and Liang *et al*., 2017), and generally isolate two discrete litter decomposition pathways for SOM formation (Cotrufo *et al*., 2015): a 'physical' path through perturbation and cryomixing to move fragmented litter particles into the mineral soil forming coarse POM, *vs* a 'dissolved' path where soluble and suspended C compounds are transported vertically through water flow and, when mineral surfaces are available, form mineral associated organic matter (MAOM). Microbial products and very small litter particles can be transported by both pathways, forming a heavy POM fraction with 'biofilms' and aggregated litter fragments around larger mineral particles (i.e., sand; Heckman *et al*., 2013; Ludwig *et al*., 2015; Buks and Kaupenjohann, 2016). Attempts to formulate these empirical observations of litter decomposition into mathematical frameworks recently culminated with development of the LIDEL model (Campbell *et al*., 2016), which in turn built upon the relationships of litter decomposition described by Moorhead *et al*. (2013) and Sinsabaugh *et al*. (2013). While the LIDEL model was evaluated against a detailed lab experiment of litter decomposition (Soong *et al*., 2015), it does not simulate SOM pools and dynamics. In nature, litter decomposition processes and SOM formation processes are necessarily coupled but are often studied and modelled separately. However, models that link litter decomposition to SOM formation are required to represent SOM dynamics in ecosystem models.

Beside the processes of leaching and fragmentation that control the two pathways mentioned above, litter decomposition processes that form SOM are governed by the balance between microbial anabolism and catabolism (Swift *et al*., 1979; Liang *et al*., 2017). A recent paradigm has emerged that emphasizes the role of microbial life strategies (e.g., K *vs* r) and carbon use efficiency (CUE) in the formation of SOM from plant inputs (Dorodnikov *et al*., 2009; Cotrufo *et al*., 2013; Lehmann and Kleber, 2015; Kallenbach *et al*., 2016). As a result, scientists have explored several approaches to represent microbes in SOM models. Research has indicated that explicitly representing microbes in a SOM model can provide very different predictions of SOM dynamics and include important feedbacks such as acclimation, priming and pulse responses to wet-dry cycles (Bradford *et al*., 2010; Kuzyakov *et al*., 2010; Lawrence *et al*., 2009; Schmidt *et al*., 2011). This research has shown that, compared to conventional models, microbially-explicit SOM models have drastically different simulated responses to environmental change (Allison *et al*., 2010; Wieder *et al*., 2015; Manzoni *et al*., 2016). However, these responses are generally validated against data at microsite spatial scales and are not necessarily generalizable over larger spatial scales (Luo *et al*., 2016).

Microbes have been explicitly represented in SOM models in many ways, from relatively simple approaches using a single microbial biomass pool or fungal:bacterial ratios (e.g., Wieder *et al*., 2013 and Waring *et al*., 2013), to more complex associations with microbial guilds or community dynamics based on dominant traits derived through genetic profiling (Miki *et al*., 2010; Allison *et al*., 2012; Wallenstein and Hall, 2012). The MIcrobial-MIneral Carbon Stabilization (MIMICS) model (Wieder *et al*., 2014) consolidated existing research at the time and uses the size of a microbial biomass pool together with Michaelis–Menten kinetics to feedback on C decay rates of SOM pools. While the MIMICS model and others (for an example see Manzoni *et al*., 2016), provide a potentially viable framework for explicitly representing microbes in a SOM model, it remains unclear whether this is practical given the lack of input data required to drive and validate these relationships (Treseder *et al*., 2012; Sierra *et al*., 2015). Furthermore, parsimony and analytical tractability are both key concerns for ecosystem models designed to operate over large spatial and temporal scales. While microbially explicit models may be essential for addressing research questions at

small spatial scales, they may introduce unnecessary, additional uncertainty to global simulations (Stockmann *et al*., 2013).

While microbial efficiency largely controls SOM formation rates, and microbial products are major components of the MAOM and the coarse, heavy POM fractions of SOM (Christensen 1992; Heckman *et al*., 2013) the long-term persistence of SOM is determined by mineral associations that are subject to saturation. Saturation limits for SOM were proposed more than a decade ago (Six *et al*., 2002) and have been supported by several empirical studies (e.g., Gulde *et al*., 2008; Stewart *et al*., 2008; Feng *et al*., 2012; Beare *et al*., 2014). Briefly, the concept of C-saturation suggests that each soil has an upper limit to the capacity to store C in mineral-associated (i.e., silt + clay, < 53µm) fractions, due to biochemical and physical stabilization mechanisms (e.g., cation bridging, surface complexation and aggregation) that are limited by a finite area of reactive mineral surfaces. While saturation kinetics are easy to define conceptually (Stewart *et al*., 2007), C-saturation as a concept has been adopted by only a few SOM models (Struc-C, Malamoud *et al*, 2009; COMISSION, Ahrens *et al*., 2015; MILLENNIAL, Abramoff *et al*., 2017). This is partly because its use in a SOM model requires a robust estimate of the specific site's saturation capacity. SOM saturation has been modelled using i) empirical regressions between silt + clay content and C concentration of that fraction (Six *et al*. 2002, as applied in COMISSION), and ii) empirical relationships between clay content and the derived 'Q_{max}' parameter of Langmuir isotherm functions (Mayes *et al*., 2012, as applied in MILLENNIAL). As noted by Ahrens *et al*. (2015), the use of C-saturation kinetics in an ecosystem model would require a map of mineral-associated C saturation capacity, and since soil C stocks in silt + clay fractions can make up the majority of total soil C stocks, a lot of weight would be put on that single driving variable for each site. However, it is worth noting that when applying C-saturation concepts, only the mineral-associated organic matter (MAOM) fraction saturates. Other SOM fractions (e.g., particulate organic matter, POM) theoretically have no saturation limit (Castellano *et al*., 2015; Cotrufo *et al*., 2018).

Attempts to consolidate the concepts of microbial control on litter decomposition and mineral control on SOM stabilization resulted in the MEMS framework (Cotrufo *et al*. 2013). To date, we are aware of only one attempt to represent MEMS within a mathematical model, the MILLENNIAL model (Abramoff *et al*., 2017). However, this model does not simulate litter decomposition explicitly and as a result does not include the impact of litter input chemistry, which is a fundamental component of the MEMS framework and needed to improve ecosystem modelling, as discussed previously.

In this study we describe and demonstrate the application of a new mathematical model (MEMS v1.0) that applies three major concepts of SOM dynamics: 1) litter input chemistry-dependent microbial CUE informing SOM formation (Cotrufo *et al*., 2013), 2) separate dissolved *vs* physical pathways to SOM formation (Cotrufo *et al*., 2015); and 3) soil C-saturation related to litter input chemistry (Castellano *et al*., 2015). The scope of this inaugural model description is limited to representing these three concepts and is not intended to include every mechanism relevant to SOM cycling. Our objective is to demonstrate the benefits of structuring a SOM model around key biogeochemical processes, rather than turnover times. Using measured SOM physical fractions from 154 forest and grassland sites across Europe (Cotrufo *et al*., 2018), key parameters were optimised to improve model performance when simulating POM-C (consisting of both light and heavy POM) and MAOM-C, under equilibrium conditions. The resulting model

was then used to test whether the behaviour of simulated SOM dynamics concur with the expected theoretical relationships. Finally, the model performance in predicting soil C stocks at equilibrium was evaluated by simulating 8192 forest and grassland sites across Europe, representing a diverse set of driving variables (i.e., climate, soil type and vegetation type).

2 Materials and Methods

2.1 Model description

The MEMS model (herein MEMS v1.0) is designed to be as parsimonious as possible while simulating the spatial and temporal scales relevant to management and policy decision making. The model is structured (Figure 1) to simulate plant litter decomposition explicitly with decomposition products defining C inputs to discrete soil pools that can be isolated with common SOM fractionation techniques (Table 1). Each state variable in MEMS v1.0 can be quantified directly using common measurement protocols and therefore calibration/evaluation data can be generated with a single fractionation scheme (Table S1). Detailed information about the model structure, the mathematical representation (i.e., differential equations) and how each mechanism is described mathematically can be found in the supplementary material. All model parameters can be found in Table 2.

MEMS v1.0 is an ecosystem-scale SOM model that operates on a daily timestep. Carbon inputs to the model are resolved for each source (in the case of multiple input streams, e.g., manure, crop residue, compost) discretely, partitioning daily C inputs between solid-phase (C1, C2, C3) and dissolved (C6) litter pools as a function of litter chemistry (nitrogen [N] content and the acid-insoluble [i.e., 'lignin'] fraction) that influences microbial decomposition processes. This structure is similar to the LIDEL model (Campbell *et al*., 2016) and follows the hypotheses that both N availability and lignin content influence decomposition by affecting microbial activity (Aber *et al*., 1990; Manzoni *et al*., 2008; Sinsabaugh *et al*., 2013; Moorhead *et al*., 2013). These input partitioning coefficients can be determined experimentally for each C input source (Table 1 & S1). Upon reaching the soil, C compounds are then subject to biotic and abiotic processes that transform and transport organic matter through an organic horizon and subsequent mineral soil layers. As described here, MEMS v1.0 currently only simulates a surface organic horizon and a single mineral soil layer, and does not yet differentiate between above- and below-ground litter input chemistry to avoid requiring additional input parameters on root litter chemistry. However, the model architecture is sufficiently generalizable to apply to multiple soil layers and/or multiple discrete sources of C input. Where possible we use the parameter names and abbreviations from the LIDEL model (Campbell *et al*., 2016).

2.1.1 Microbe mediated transformations and dissolved organic matter (DOM) production

Many of the biogeochemical processes represented by MEMS v1.0 are assumed to be microbially mediated (and therefore result in exo-enzyme breakdown and CO_2 production), but only two lead to C assimilation into a distinct microbial biomass pool – from the water-soluble and acid-soluble litter pools (C1 and C2, respectively). In the mineral soil, microbial anabolism and catabolism are implicit and considered part of the turnover of each pool. The C transferred from the C1 and C2 litter pools into microbial biomass is defined by a dynamic CUE parameter controlled by the N content of the input material and the lignocellulose index (LCI; defined as the ratio between acid-insoluble to the sum of acid-soluble + acid-insoluble) of the litter layer (i.e., lower CUE results when a higher proportion of the

litter is acid-insoluble). The lack of C transferred from other pools into microbial biomass implies their decay from co-metabolism with the more labile C sources (i.e., Klotzbucher *et al*., 2011; Moorhead *et al*., 2013). Once assimilated within microbial biomass, the anabolism of microbial activity results in generation of microbial products (i.e., necromass) that form tightly bound aggregates of biofilms and small litter fragments around sand-sized soil particles (Huang *et al*., 2006; Buks and Kaupenjohann, 2016), and dissolved organic matter (DOM). These contribute to the heavy POM (C5) and litter DOM (C6) pools, respectively. While these processes are well supported by relevant literature, to retain parsimony MEMS v1.0 represents microbial metabolism processes implicitly as per their description in LIDEL.

Even though not all pools explicitly produce microbial biomass, all pools do produce DOM. Recent studies have shown that DOM and small suspended particulates result from the decomposition and fragmentation of all forms of inputs including those characterized as 'inert', such as pyrolized material (Soong *et al*., 2015). Consequently, the model assumes that all microbially-mediated decomposition produces some C in DOM with rates specific to the pool from which the C originates. Since DOM generation is strongly influenced by the elemental composition of the litter material (Soong *et al*., 2015), it is intrinsically linked to microbial CUE, employing the same formulation as LIDEL, which accounts for input N content and LCI of the litter layer (Campbell *et al*., 2016). At present, root exudation is not explicitly represented but the presence of a soil DOM pool (C8) will allow for incorporation of root exudation processes in later versions.

2.1.2 Perturbation and physical transport

While microbial activity directly influences DOM production and therefore its transport with water flow (pool C8), the physical pathway to SOM formation (i.e., forming pools C5 and C10; POM) results from perturbation and fragmentation processes (Cotrufo *et al*., 2015). The exact mechanisms of perturbation are hard to generalize over the globally diverse conditions that an ecosystem scale model such as MEMS v1.0 is designed to operate. Consequently, the litter fragmentation and perturbation rate (LIT_{frg}) in MEMS v1.0 is represented as a first-order process where the default value of LIT_{frg} was informed by empirical estimates (e.g., Scheu and Wolters, 1991; Paton *et al*., 1995; Yoo *et al*., 2011); but uncertainty can be reduced by relating this rate to specific site conditions that reflect, in particular, soil macro- and mesofauna activity. The division of litter fragmentation between the C5 and C10 pool is derived from fractionation results that separate the light and heavy POM. The split between these two fractions appears to vary with land use (Poeplau and Don, 2013), although the exact relationship is unclear. Consequently, MEMS v1.0 applies an average over all land uses. Particulate organic matter is divided between a heavy and a light pool because recent evidence suggests the two fractions are differentially influenced by temperature and management linked to aggregation and land-use change (deGryze *et al*., 2004; Tan *et al*., 2007; Poeplau *et al*., 2017). Furthermore, the heavy, coarse POM pool can play an important role in soil nutrient cycling (Wander, 2004) and it has a different turnover time to either the MAOM or light POM fraction (Crow *et al*., 2007; Poeplau *et al*., 2018).

2.1.3 Liquid phase transport

Vertical transport of DOM can be simulated as a function of water flow in a process-based soil hydrology model. However, in this first, standalone version, MEMS v1.0 assumes that DOM is transported rapidly downward through percolation and advection according to a constant water flux. As with the LIT_{frg} parameter, the rate of vertical C

transport (controlled by parameter DOC_{frg}) would ideally be site-specific, but is currently fixed at a general, default value informed by relevant literature (Trumbore *et al*., 1992; Kindler *et al*., 2011). More information can be found in the supplementary material and in Table 2.

2.1.4 Sorption and desorption with mineral surfaces

The organo-mineral complexes that define a large portion of MAOM-C in MEMS v1.0 operate under the principles of Langmuir isotherms, which have also been used in the COMISSION and MILLENNIAL models (Ahrens *et al*. (2015) and Abramoff *et al*. (2017), respectively). These isotherms represent a net C transfer between soil DOM (pool C8) and MAOM (pool C9) that encapsulates all sorption mechanisms (e.g., cation bridging, surface complexation, etc.). While MEMS v1.0 uses the same general Langmuir saturation function as the MILLENNIAL model, it estimates maximum sorption capacity (parameter Q_{max}) differently. Here, we use sand content to derive the maximum C concentration of the silt + clay fraction according to a regression calculated by pooling all soils data reported by Six *et al*. (2002). This is then converted to C density using the site-specific soil bulk density provided as a driving variable to the model.

In addition to the Q_{max} parameter, the isotherm saturation function also relies on an estimate of a specific soil's 'binding affinity' (parameter K_{lm}). Typically, this is a product of a soil's specific mineralogy, influencing the type of organo-mineral bonds that are formed and the strength of those bonds (Kothawala *et al*., 2009). Furthermore, the type of C compounds being sorbed are also key to defining an isotherm's binding affinity (Kothawala *et al*., 2008; Kothawala *et al*., 2012). This parameter can be very difficult to generalise without requiring exhaustive information on soil physiochemical conditions (e.g., clay type, Fe/Al concentration, etc.), but the work of Mayes *et al*. (2012) presented an empirical relationship between K_{lm} and native soil pH, with pH acting as a proxy for mineralogical conditions. This relationship (derived from isotherms calculated for 138 soils of varying taxonomies) provides a good starting point for estimating K_{lm} and is also used by the MILLENNIAL model (Abramoff *et al*., 2017). It is worth noting that desorption is implicit in the Langmuir saturation function used by MEMS v1.0 (unlike the explicit representation in COMISSION, Ahrens *et al*., 2015), meaning that when the MAOM pool reaches saturation the net transfer from soil DOM to MAOM may be negative and C is transferred from MAOM to DOM. The simulated sorption–desorption processes in MEMS v1.0 are directly derived from empirical data and are similar to other SOM models (Wang *et al*., 2013; Ahrens *et al*., 2015; Dwivedi *et al*., 2017).

2.1.5 Heterotrophic respiration and controls on microbial activity

Aside from the litter layer DOM (pool C6), each of the state variables in MEMS v1.0 decay with unique specific maximum rates, with the resultant C flux being partitioned into CO_2 (aggregated into the C7 sink term) and an accompanying decomposition product flux into other pools, mainly DOM. Thus, the decay rate constants represent total mass loss potential, embodying DOM-C generation as well as CO_2 emissions, as per a recent decomposition conceptualization (Soong *et al*., 2015). While the maximum specific decay rates for most pools are fixed parameters informed by empirical data (Table 2), several studies suggest linking decay rates of recalcitrant compounds to those of more microbially-accessible compounds (Moorhead *et al*., 2013; Campbell *et al*., 2016). This follows similar hypotheses to the priming effect, that chemically recalcitrant compounds (e.g., lignin, cutin and suberin) are processed co-metabolically when microbes act preferentially on more energetically favourable compounds nearby (Carrington

et al., 2012; Větrovský *et al*., 2014). Consequently, MEMS v1.0 applies this through use of the same functions as those used by the LIDEL model (Campbell *et al*., 2016), estimating the maximum specific decay rate of pool C3 with a relationship to parameter k_2 (i.e., the maximum specific decay rate of the acid-soluble litter fraction, pool C2). At present, CO_2 emitted from soil mineralization of DOM is associated with the values presented in Kalbitz *et al*. (2005).

2.1.6 Decay rate modifiers

Temperature is used as the main environmental control on maximum specific decay rates of each pool. The rate modifying function used by MEMS v1.0 is adapted from that of the StandCarb model (Harmon and Domingo, 2001). This function is consistent with empirical data and enzyme kinetics, implying that microbial decomposition rates peak at an optimum temperature with reduced rates above and below. Coefficients that define the function also include the Q_{10} and reference temperature for that specific pool. Therefore, the function can utilise empirical data if available for a site. This is a relatively simple function that only accounts for temperature. Simulating the influence of other controls on decomposition, such as water, oxygen and nutrients, are beyond the scope of this inaugural version of the MEMS model but will be incorporated in future development.

2.1.7 Model implementation and driving variables

MEMS v1.0 is a series of ordinary differential equations solved for discrete time steps by numerical integration using finite differencing techniques from the Runge-Kutta family of solvers. Implementation is performed through the deSolve package (Soetart *et al*., 2010) written for R (all equations and associated detail can be found in Supplementary Information). Parameters used to solve MEMS v1.0 are described along with their default values and associated references in Table 2.

Initializing MEMS v1.0 requires basic site characteristics (climatic and edaphic conditions as well as land management information) and ideally uses measurements of daily C input. However, C inputs are rarely available at daily time scales. Consequently, for this inaugural version of the MEMS model we employ a simple function to interpolate daily C inputs from annual Net Primary Productivity (NPP), partitioning aboveground/belowground and to the simulated soil layer using land-use specific root:shoot ratios and a simple root distribution function (Poeplau, 2016). Details of these approaches are given in the supplementary materials and all required driving variables are shown in Table 3. Since the major C pools can each be quantified using common analytical methods (Table 1; Table S1), the best way of initializing the size of these pools in MEMS v1.0 is to use measured data. However, when measured data are not available, a typical site simulation employs a spinup that runs the model to steady-state conditions based on average climatic and edaphic conditions, as well as average C inputs.

2.2 Global sensitivity analysis

The default parameter values (i.e., those governing C turnover and fluxes between pools) used by MEMS v1.0 are informed by data from relevant literature (Table 2). However, different studies may suggest different values based on discrete site conditions, meaning *a priori* estimates may not necessarily be generalizable across all sites that the model could simulate. A variance-based global sensitivity analysis was performed to determine each parameter's relative contribution to the change in each state variable (i.e., determining which parameters have the largest influence on the size of each model pool). The sensitivity analysis was repeated for different simulation lengths (1 – 1000 years) as

different fluxes operate at different temporal scales, thereby meaning that the relative importance of each parameter changes through time. Initial pool sizes were set to 0 and the model was initialized to simulate a steady-state scenario based on average site conditions (derived from ~8000 forest and grassland sites in the Land-Use/Land Cover Area Frame Survey (LUCAS) dataset ([Toth *et al*., 2013] – see Table 3). Note that all temperature modifier parameters (T_{ref}, T_{opt}, T_{Q10}, T_{lag} and T_{shp}; Table 2) were excluded in this sensitivity analysis as the resulting T_{mod} has the same effect on all decay rates. Maximum and minimum values of all other parameters (n = 24) were defined as 50% above and below the literature-derived (baseline) value (Table 2). Using Latin Hypercube techniques to sample within the full parameter space, a global sensitivity varying all parameters was used to determine total variance for changes to each model pool. Then, in turn, each individual parameter was fixed at its baseline value while all others varied. This defines the contribution to a pool's variance from each parameter, averaged over variations in all other parameters (Sobol, 2001; Saltelli *et al*., 2008). When normalized over the global sensitivity variance, a contribution index provides the proportion of variance explained by each parameter. The analysis was run 10,000 times to define the total parameter space and the whole procedure was repeated annually for simulation lengths between 1 to 1000 years.

2.3 Model response to changes in driving variables

To determine the model's steady-state response to changes in each individual driving variable, a local one-at-a-time (OAT) sensitivity analysis was performed by sequentially simulating different equilibrium conditions for 1000 years. The baseline estimates for edaphic inputs, temperature and C input quantity were informed by the LUCAS dataset ([Toth *et al*., 2013] – see Table 3 and below for more details), with mean values defining the mid-points and ranges defined as the minima and maxima. Litter chemistry driving variables were adapted from the ranges described by Campbell *et al.* (2016). Note that while typically described as a sensitivity analysis, an OAT approach is not as robust as variance-based techniques because it cannot determine interactions between input variables. However, OAT results are easier to interpret as there are no confounding impacts and relationships observed are solely a result of changing one variable. Additionally, we assess the model's qualitative relationships between driving variables by comparison to a study by Castellano *et al*. (2015); combinations of high/low sand content and high/low soil pH were used to examine whether model projections agree with the hypothesized relationships between input litter chemistry and MAOM-C stocks at steady state. In these scenarios, Alfalfa (*Medicago sativa*) and Ponderosa Pine (*Pinus ponderosa*) were used as examples of a high- and low-quality litter input, respectively, with litter chemistry driving variables adopted from Campbell *et al*. (2016).

2.4 Parameter optimization

2.4.1 LUCAS dataset and soil fractionation data

Parameter optimization for MEMS v1.0 used data from the LUCAS dataset (Toth *et al*., 2013). This dataset contains basic soil properties including C data for almost 20,000 sites across Europe, sampled in 2009, representing a wide spatial range over 25 countries with diverse gradients of soil types, climates and land uses (Figure S1). Complimented with geo-referenced estimates of annual NPP from MODIS satellite data (ORNL DAAC, 2009), and daily temperature data from the Climate Prediction Center's Global Temperature (CPC-GT) database (NOAA, 2018), this provided all driving variables required to run MEMS v1.0.

A representative subsample (Figure S2) of forest and grassland sites from LUCAS were selected for fractionation to generate data for POM and MAOM pools (see Cotrufo *et al*., 2018). Specifically, topsoil (0-20 cm) samples from 78 grassland sites and 76 forested sites were fractionated by size (53 µm) after full soil dispersion in dilute (0.5 %) sodium hexametaphosphate with glass beads on a shaker (see Cotrufo *et al*., 2018 for more details). The fraction passing through (< 53 µm) was collected as the MAOM, while the fraction remaining on the sieve was collected as the POM. It is worth noting that this fractionation did not separate the POM into a light and a heavy POM, as represented in MEMS v1.0 (i.e., C5 and C10), thus these model fractions were combined for data-model comparisons (see below). After drying to constant weight in a 60 °C oven, each fraction was analysed for C and N concentration in an elemental analyser (LECO TruSpec CN). Samples from sites with a soil inorganic C content greater than 0.2 % (as reported in the LUCAS database) were acidified before elemental analyses to remove carbonates, so that the %C of each fraction represented the organic C only. Carbon concentrations of each fraction and the total soil organic carbon (SOC) were converted to stocks for the top 20 cm soil layer using bulk density estimates reported with the LUCAS database. A georeferenced summary of these 154 sites can be seen in Figure S2 and summary information of the fractionation data and comparisons between land use classes is shown in Figures S3 and S4.

2.4.2 Optimization procedure

Informed by the global sensitivity analysis, four parameters accounted for ~60 % of the variation in steady-state bulk (and MAOM/total POM) soil C stocks. These were *Nmid*, *k5*, *k9* and *k10* (see Table 2 for details) and were used for optimization to improve model performance. Maximum and minimum values representing realistic ranges of each parameter were informed by relevant literature and rounded to appropriate boundaries (Table 2; Table S2): *Nmid* (0.875, 2.625), *k5* (6.0^{-5}, 1.0^{-3}), *k9* (1.0^{-5}, 4.0^{-5}), *k10* (1.0^{-4}, 1.0^{-3}). These values set the limits for Latin Hypercube sampling to define 1024 unique parameter sets that, together, span the full range of each parameter. The fractionated LUCAS site data was used to train and test the model, applying a repeated *k*-fold cross-validation approach (Kuhn and Johnson, 2013) to identify best parameter values for the full variation of conditions at all 154 sites. Comparisons were made between measured soil C stocks and those resulting from steady-state simulations for each site. Of these sites, 120 (78 %) were used for training and the remaining 34 (22 %) were used for testing. Root mean squared error (RMSE) was applied as the objective function. Using the training results, the set of parameters that reported the lowest RMSE for each fraction was used to ensure this 'best' parameter set also performed well (i.e., RMSE was within 10 % of that reported for the training sites) against the 34 sites of measured data withheld for testing. This process was repeated 10 times using different subsets of the 154 sites for training and testing (i.e., 10 'folds' in the cross-validation approach).

To determine the optimized parameter values, the parameter set that reported the lowest RMSE for each subset of training sites (i.e., each fold) was selected and values from all 10 folds were averaged. Optimized values differ depending on which measured fraction is compared to model predictions (whether comparing pool C9 to measured MAOM-C, the sum of pools C5 and C10 to measured total POM-C, or the sum of pools C5, C8, C9 and C10 to measured bulk SOC). The new, optimized parameter values were derived from the averaging of those that minimized RMSE when compared to the MAOM fraction. This was chosen (instead of those optimized for POM or bulk SOC) since the MAOM fraction is typically the largest single soil C pool and using this approach led to the biggest overall decrease in RMSE when compared to all available data (Table S2).

2.5 Model evaluation for forests and grasslands in Europe

Having optimized key parameter values, the new global parameter set for MEMS v1.0 was used to simulate the remaining forest and grassland sites of the LUCAS dataset for independent evaluation. Driving variables of edaphic conditions and land-use type were extracted for each site from LUCAS and combined with daily estimates of C inputs and temperature (derived from MODIS annual NPP data and CPC-GT daily maximum and minimum air temperature data, respectively). Where these data were unavailable, the site was removed from further evaluation. Three forest land-use classes (as described in LUCAS) were included, along with the pure grassland land-use class. This resulted in a final dataset of 8192 sites (3487 grasslands, 1713 coniferous forests, 1590 broadleaved forests and 1402 'mixed' forests). Mixed forests are defined to contain coniferous and broadleaved species that each contribute > 25% to total tree canopy. Summary information for these sites can be found in Figure S1. To differentiate between input litter chemistry, root:shoot ratios and root distribution of the four land-uses, generic driving variables for each were derived from relevant literature. Details of these inputs are shown in Table 3.

Each of the 8192 sites was initialized with zero pool sizes and simulated for 1000 years to achieve steady state conditions. This assumed the same intra-annual distribution of daily temperature and C input for each year. Organic carbon content reported in LUCAS was converted to SOC stock using the estimated bulk density reported with the database and reduced according to the measured rock/gravel content (Equation 1).

$$SOC = C_{conc} * {}^{L}\rho * (1 - {}^{L}rock) \quad (1)$$

Where SOC is soil organic carbon stock in Mg C ha^{-1}, C_{conc} is the measured C content in percent, ${}^{L}\rho$ is the bulk density of soil layer L in g cm^{-3} and ${}^{L}rock$ is the rock content of soil layer L expressed as a fraction. This total SOC stock, was compared to MEMS v1.0 model output. Model performance was evaluated for several classes of environmental conditions, with sites divided into above and below median values of mean annual temperature (MAT, 8.3 ºC), mean annual precipitation (MAP, 687 mm), annual NPP (647 gC m^{-2} yr^{-1}) and sand content (50 %), for each land-use type. Several standard metrics for error and bias were used to evaluate model performance following the flowchart presented in Smith *et al.* (1997), including Mean Absolute Error (MAE), Mean Bias Error (MBE), Root Mean Square Error (RMSE), modelling efficiency (EF), and Coefficient of Determination (CofD). Additionally, we use 16 environmental classes to derive an estimate of measurement uncertainty based around sites of similar conditions (e.g., hot, wet, low input, sandy soil) for each land use. To include both measurement and simulation error in the same evaluation metric, we applied a modified *F*-test statistic that uses lack-of-fit sum of squares to account for both experimental and prediction uncertainty (see Sima *et al.*, 2018 for more information). The variance required to calculate these was derived by using the full number of environmental classes as described above (n = 16). Due to the lower number of fractionated sites in each group, only temperature and sand content were used as environmental classes (i.e., n = 4) to evaluate performance at these 154 sites. One-way ANOVAs were performed to show where average model results were significantly different from average measured C stocks. An α level of 0.05 was used to determine the significance of the ANOVA and *F*-tests. Finally, we also use the standard errors for bulk topsoil C stocks of each environmental class to determine the significance of RMSE assuming a two-tailed Student's t distribution and 95% confidence interval, as described by Smith *et al.* (1997). All data processing and statistical analysis was performed in R (v3.4; R Core Modelling Team, 2018).

Biogeosciences Discuss., https://doi.org/10.5194/bg-2018-430
Manuscript under review for journal Biogeosciences
Discussion started: 17 October 2018

3 Results

3.1 Sensitivity and behaviour of MEMS v1.0

3.1.1 Parameter sensitivity at different timescales

Bulk SOC stocks were sensitive to different sets of parameters depending on the duration of the simulation (Figure 2). Parameters that define litter fragmentation and perturbation rates (*LITfrg*) or microbial CUE (mainly *LCmax*, *Nmax* and *Nmid*) are responsible for rapid (< 2 years) changes in C stocks, particularly those in the litter layer and light POM. As simulation time increases, the influence of these parameters declines relative to the litter and POM decay rate parameters, particularly *k5* and *k10*. Fifty years after simulations are initialized, more than 75% of the sensitivity in total soil C stock was due to the maximum specific decay rate of light POM (i.e., parameter *k10*). After this point, its relative contribution to total C stock sensitivity diminishes as the parameters that define MAOM-C sorption become more important (i.e., coefficients that determine the regression to calculate MAOM-C saturation capacity [*scIcept* and *scSlope*]). Overall, our sensitivity analysis showed that the expected dynamics with different processes (e.g., litter fragmentation, microbial processing and sorption) are operating at the appropriate timescales to structure SOM dynamics, and their associated parameters are more, or less, important depending on the initial pool sizes and model run/experiment duration. Figure 2 can be interpreted as a depiction of how each pool of MEMS v1.0 accumulates over time.

3.1.2 Soil carbon response to changing environmental conditions

Alone, each driving variable (edaphic conditions, temperature, and input litter quantity/quality) in MEMS v1.0 has a discrete and non-linear relationship to the proportion of soil C stored in the MAOM and POM pools under steady-state conditions (Figure 3). This analysis alters only one driving variable at time while holding others constant at an average value. Bulk C stocks are predicted to be mostly MAOM in all cases except when C inputs (*annNPP*) are very high (i.e., > 1.5 kg C m^{-2} yr^{-1}; Figure 3). This results from the fact that the MAOM pool will saturate at high input rates whereas the POM pools do not (Castellano *et al.*, 2015; Cotrufo *et al.*, 2018). Sand content and soil pH influence a site's MAOM saturation capacity, and therefore a low capacity (i.e., high sand content) with mineralogy associated with weaker organo-mineral bonding (i.e., high soil pH) has proportionally more total POM. Litter input chemistry variables also have different, and sizable, impacts on whether SOM forms and persists primarily in MAOM or in POM (as denoted by the MAOM:POM ratio). Note that POM in the MAOM:POM ratio refers to total POM (i.e., pools C5 and C10 combined). The fraction of litter input that is hot-water extractable (*fSOL*) is a key determinant of MAOM formation rates and when *fSOL* is high, MAOM-C stocks at steady state are predicted to be more than 4 times higher than POM-C stocks (Figure 3). Conversely, when input material has a high acid-insoluble (*fLIG*) content and a low N content (*LitN*) the size of the organic horizon increases and, over time, POM-C stocks approach a 1:1 ratio with MAOM-C stocks. Figure 3 shows the impact of one driving variable while all others remain constant. When many of these inputs vary at the same time, the relationships to MAOM:POM can be very different (for example, the model predicts twice as much POM-C as MAOM-C when simulating a sandy soil with coniferous vegetation and high *annNPP*).

MAOM-C saturation in the model is largely dependent on an interaction between the quantity of C inputs, the soil texture (i.e., sand content) and mineralogy (i.e., for which soil pH is used as a proxy). Figure 4 shows that our mathematical formulation of sorption to mineral surfaces generated a very similar relationship to that proposed by Castellano *et al*. (2015). When C inputs are low, litter input chemistry has the greatest influence on the MAOM-C stock under steady-state conditions. This is particularly true in soils with the strongest mineral bonding (i.e., low pH) and high sorption capacity (i.e., low sand %; Figure 4 top right panel).

3.2 Improved simulation due to parameter optimization

Initial parameter values derived from relevant literature provided good estimates judging from model performance with measured fractionation data (Table S2). Prior to optimisation, the difference between measured and modelled bulk soil C stocks of fractionated LUCAS sites was insignificant for all four land-uses (one-way ANOVA, $p > 0.05$). However, accounting for experimental and simulation uncertainty (variance calculated by four groups: divisions of high/low mean annual temperature and sand content) MEMS v1.0 only accurately described bulk SOC stocks for the grassland land-use class (*F*-statistic < 0.05). After optimisation, overall model fit with all soil C fractions (MAOM, total POM and bulk) was improved by increasing the maximum decay rate of MAOM (parameter *k9*) and decreasing the maximum decay rate of light POM (parameter *k10*), the maximum decay rate of coarse, heavy POM (parameter *k5*), and the inflection point for the logistic curve that defines the N effect on microbial CUE (parameter *Nmid*). This resulted in a lower RMSE against all measured data compared to baseline values (Table S2). Despite the improved model fit, the error in simulated values for broadleaved forest sites was still more than the error inherent to the measured data (at a 95% threshold and as defined by the modified *F*-test from Sima *et al*., 2018). This was primarily caused by two sites where measured total POM-C stocks were reported to be > 95 Mg C ha^{-1} in the top 20 cm (Figure 5). When these sites were removed from statistical comparisons there were no significant differences between modelled and measured bulk SOC stocks for any land use class.

Measured fractionation data from the four major land-use classes showed a wide range of soil C stocks and a significantly different MAOM:POM ratio between grassland and forests (Figure 5; Figure S4). This was predominantly due to grassland topsoil (0-20 cm) having more MAOM and less total POM, compared to coniferous soils (Figure S3). On average, simulations of the fractionated sites agreed well with measured data, demonstrating no significant differences ($p > 0.05$) between measured and modelled C stocks of total POM or bulk soil for all land uses, and for MAOM at broadleaved, mixed and coniferous forest sites (Figure 5). The only statistically significant difference was between measured and modelled MAOM-C stocks for grassland sites ($p < 0.01$). However, measurements have a considerably larger range between minimum and maximum values than did model simulations, particularly for total POM, which largely explained the high overall RMSE when comparing all 154 sites (Table S2).

3.3 Model evaluation for forests and grasslands in Europe

Despite only including a few of the many factors that influence SOM dynamics, MEMS v1.0 was able to capture the expected relationships between site conditions and total mineral soil C stocks based on an evaluation of the optimized model with independent data (Figure 6). Mean absolute error over all sites (n = 8192) was low (MBE = 1.1 MgC ha-

498 [1]) and CofD was above 1, indicating that the simulated C stocks capture the trend of the measured data better than the
499 mean of the measurements (Table 4). The main lack of fit was observed as the model consistently underestimated
500 bulk soil C stocks in forest systems with low mean annual temperature (MAT < 8.3 ºC) and sandy soil textures (sand
501 content > 50 %). When divided by land-use classes, grassland sites had the lowest residuals and mixed forest sites
502 had the highest (Figure 6). Using low and high divisions of MAT, MAP, sand content and C input quantity, to account
503 for variance between each of these groups (n=16), RMSE indicated that the model predictions of C stocks fell within
504 the 95 % confidence interval of the measurements for coniferous and mixed forest sites. Using the same groups but
505 also accounting for simulated variance indicated that the accuracy of MEMS v1.0 predictions were statistically
506 significant for all land uses besides broadleaf forest sites (F-statistic > 0.05; Table 4). A geographic analysis of model
507 performance indicated that the model performed best across France and Northeastern Europe but poorly across the
508 UK, Ireland and Southern Sweden (Figure 7). Furthermore, topsoil C stocks of broadleaved sites in Southeastern
509 Europe, particularly Romania, were consistently overestimated by the model, especially when sites had low MAP
510 (Figure 6; Figure 7).
511
512 In general, discrepancies between measured and modelled values were largest for the broadleaved forest land use
513 class. Results from analysis of the fractionated sites suggest that the model cannot achieve the very high POM-C
514 stocks measured at some sites. Optimized parameter values aim to produce a good overall model fit but are unlikely
515 to be able to capture the full range of measured values (for example, the lowest bulk topsoil C stock for a broadleaved
516 site was 7 Mg C ha^{-1} whereas the highest was 218 Mg C ha^{-1}). A summary of model performance against these 8192
517 evaluation sites is shown in Table 4.

Biogeosciences Discuss., https://doi.org/10.5194/bg-2018-430
Manuscript under review for journal Biogeosciences
Discussion started: 17 October 2018

4 Discussion

MEMS v1.0 was designed to consolidate recent advances in our understanding of SOM formation and persistence into a parsimonious, ecosystem-scale, mathematical model that can be developed further and implemented in Ecosystem and Earth System model applications. In this study we aimed to provide proof-of-concept that a model structure built around known biogeochemical mechanisms (Figure 1) and measurable pools could be advantageous for application over varied site conditions. Another advantage of using this novel structure is that each aspect is empirically quantifiable, allowing for straightforward model evaluation of both total and fractionated SOM, addressing a common concern among conventional SOM models (Campbell and Paustian, 2015).

4.1 Sensitivity and behaviour of MEMS v1.0

The relationships between model driving variables and soil C stocks at steady-state highlight the importance of litter chemistry on relative proportions of MAOM and total POM in MEMS v1.0 (Figure 3). This is generally because both POM pools accumulate C when input litter has a high acid-insoluble fraction and a low N content, resulting from reduced microbial accessibility and reduced DOM production (Scheibe and Gleixner, 2014). This trend is also common in empirical studies and often associated with land-use change from herbaceous to woody vegetation (Filley *et al*., 2008). Many of the parameters that influence the processes of POM formation and persistence (e.g., *LITfrg*, *Nmid*, *LCImax*, etc.) have relatively high importance (i.e., sensitivity) to changes in total SOM within relatively short time frames (i.e., < 10 years; Figure 2). This captures an important real-world trend that POM is typically more vulnerable to decomposition with disturbance compared to MAOM (Cambardella and Elliott, 1992). Consequently, the model is able to simulate this impact with processes and associated parameters operating at the appropriate time-scale.

One main objective of structuring MEMS v1.0 around empirically-defined biogeochemical processes is so that it can accurately represent the timescales on which different processes operate, rather than being solely dependent on turnover times of conceptual pools. This is particularly relevant given our new understanding that the MAOM fraction has short-term dynamics (Jilling *et al*., 2018). Consequently, it is reassuring to see that this knowledge, which is incorporated into the MEMS v1.0 design, can be seen in Figure 2, where the parameters that operate on short time-scales also have an immediate impact on the MAOM pool given the complexity of controls in the model structure. The model's agreement with the hypothesized relationship from Castellano *et al*. (2015) is also reassuring, and represents an important proof of concept that associates litter chemistry and C saturation capacity with MAOM-C stocks at steady-state (Figure 4).

4.2 Model evaluation of MEMS v1.0

While average agreement between measured and modelled soil C stocks was very good for MEMS v1.0, the model failed to capture the wide range in total POM-C stocks that were observed at the fractionated LUCAS sites (Figure 5). This may be because this first version of the model does not include several of the key controls on POM dynamics, such as aggregation (Gentile *et al*., 2011), activity of soil fauna (Frouz, 2018) and nutrient availability (Bu *et al*., 2015; Averill and Waring, 2018). Furthermore, very few of the sites will likely be under true steady-state conditions leading to further discrepancies between model predictions and measured values.

When examining the comparison between measured and modelled bulk soil C stocks for the 8192 forest and grassland sites, residuals were particularly large for high latitude forestry sites in southern Sweden and the UK (Figure 7). We hypothesize that this is primarily due to the fact that MEMS v1.0 does not simulate soil moisture controls on decomposition, and temperature effects are applied through a simple function. In reality, these sorts of forest soils are known to have very high total POM-C stocks, resulting from decades of consistent inputs and cold, wet climates resulting in low decomposition rates (Berg, 2000). Differences between measured and modelled soil C stocks are also likely due to uncertainties with driving variables and specifically the MODIS estimates of NPP. The 2009 NPP data from MODIS were used to estimate the C inputs to soils in our simulations, and these data may not be representative of the average historical C inputs for those sites, which would impact the observed amounts of soil C.

4.3 Improving the parameters of MEMS v1.0

The current iteration of the MEMS model is not intended to be able to simulate all scenarios and environmental conditions, but this study indicates it can be reasonably accurate in simulating forest and grassland sites in Europe under steady-state conditions (Figure 6; Table 4). That said, several of the parameters in MEMS v1.0 are either poorly constrained or loosely defined in the current model. The *LITfrg* parameter, for example, defines a fixed litter fragmentation and perturbation rate that transfers C from the structural litter pools (C2 and C3) belowground (to C5 and C10). The global sensitivity analysis of MEMS v1.0 indicates that *LITfrg* is particularly important for several model pools and total SOC early in a simulation (Figure 2). There are several areas of research that may help make this process more mechanistic in MEMS and allow for feedbacks with site conditions (e.g., Scheu and Wolters, 1991; Yoo *et al*., 2011). One option to generalise the vertical transport of structural litter into the soil may be to apply a diffusion approach that can be valid at the ecosystem scale, as described in the SOMPROF model (Braakhekke *et al*., 2011). More empirical data to link site conditions to perturbation processes (e.g., cryoturbation, bioturbation, churning clays) would help with this area of MEMS model development.

As with vertical distribution of physical SOM, the transport of DOM vertically between layers lacks a mechanistic foundation in MEMS v1.0. A noteworthy approach that attempts to simulate this transport while also representing bioturbation through diffusion and sorption-desorption processes is presented in the COMISSION model (Ahrens *et al*., 2015). While these models apply more mechanistic functions to represent these key processes, one can debate whether the increased complexity and computational demands are necessary. This, of course depends on the model objectives and in MEMS v1.0 we have prioritised parsimony and deliberately minimised the number of algorithms and parameters. While the model cannot yet address hypotheses about litter fragmentation or DOM leaching, the generic structure of MEMS v1.0 can incorporate these processes in a more explicit manner in future versions.

Additional parameters of MEMS v1.0 that are poorly constrained include those associated with the LIDEL model. These parameters (specifically those related to DOM generation and microbial assimilation, see Table 2) were estimated using Bayesian analysis that employed empirical data (Soong *et al*., 2015), but resulted in large posterior distributions with high uncertainty as noted by Campbell *et al*. (2016). Consequently, more data is required from different litter types to help constrain these parameter values. In particular, the amount of DOM leached from decaying microbial biomass (parameter la_2) is particularly important for MAOM formation when the pool is relatively small (< 25 years in Figure 2). MEMS v1.0 currently uses the estimated value from Campbell *et al*. (2016) for this parameter

(0.19 g DOM g decayed microbial biomass^{-1}) but it is worth noting the reported posterior interval width was more than double this value (0.398 g DOM g decayed microbial biomass^{-1}). Similarly, the rate of microbial product generation from microbial biomass (parameter *B3*) was seen to be even more variable (Campbell *et al*., 2016). Empirically, the rate that microbial products are generated from microbial turnover is highly variable depending on the microbial community and the site conditions (Xu *et al*., 2014). While improving these parameters was outside the scope of this study, the path towards improved model performance can be addressed with new empirical data that better inform the model parameters.

4.4 Opportunities for further development in MEMS v1.0

In its current capacity, MEMS v1.0 is limited in scope regarding the land use scenarios it can simulate accurately. Specifically, the initial model does not simulate the hydrological or nitrogen cycles, and currently operates on a single soil layer. However, MEMS v1.0 has been built to have a modular architecture, with careful consideration given to how additional processes can be addressed through future model development.

The relationship between C and N in soils is fundamental to SOM dynamics (McGill and Cole, 1981), and therefore simulating the N cycle is at the forefront of plans to develop in the MEMS model. Since the MEMS model structure is based on soil fractions that can be physically isolated, each current soil C pool in MEMS v1.0 (i.e. pools C5, C8, C9 and C10) can also have a direct equivalent for N, and be consistent with the fractionation scheme for the C dynamics (Table S1). However, additional pools of nitrate and ammonium (and associated mechanisms to describe N- fixation, nitrification and denitrification) are needed to accurately describe plant-soil nutrient feedbacks. This highlights a major objective of future MEMS model development, i.e., to ensure the model can be easily coupled with existing modules that describe other aspects of the ecosystem (e.g., plant growth routines).

Another key feature of MEMS v1.0 is its ability to test specific hypotheses directly against empirical data, such as effects of soil priming on soil C stocks, effects of microbial feedbacks on OM sorption to mineral surfaces, or the effects of soil fauna on SOM formation. Because each of the existing model pools can be isolated physically and quantified, the rates of flux between these pools can also be quantified with isotopic tracer studies. Not only does this mean parameterization and evaluation data can be generated easily, but also that experiments can be designed with this mathematical framework in mind, specifically generating the data required to develop, evaluate and improve the model. While the current scope of MEMS v1.0 does not address all climate-C feedbacks, it does provide the basis for a more mechanistic model that can simulate SOM dynamics at the ecosystem scale.

5 Conclusions

As a carbon model designed around the processes that govern SOM formation, MEMS v1.0 provides an analytically tractable framework that can be used to test specific hypotheses by pairing empirical experiments with model simulations. While the inaugural version of this new model has limitations for direct evaluation with real-world measurements, on average, its performance with simulating steady state conditions equates well with topsoil C stocks measured for ~8000 forest and grassland sites across Europe. Using a structure that aligns with our contemporary understanding of soil C dynamics, we also show that MEMS v1.0 is capable of accurately proportioning SOM between

particulate and mineral-associated fractions by accounting for litter chemistry of the input material. By using litter chemistry to inform SOM formation pathways and edaphic conditions to inform the C-saturation capacity of a soil, MEMS v1.0 also shows consistent trends with experimental findings.

Next steps for MEMS model development will require detailed routines of N and hydrological cycling, as well as additional external drivers of SOM dynamics (e.g., land management practices). To reliably incorporate these aspects in the MEMS model will require effective collaboration between modellers and experimentalists to design studies that can both i) elucidate the underlying mechanisms that MEMS is built upon and ii) generate the parameterization and validation data required to reduce model uncertainty. Successful execution of this strategy will advance development of an ecosystem scale model that can improve assessments of management and policy action on sustainability of soils and associated ecosystem services.

Code and data availability

The LUCAS dataset can be found at https://esdac.jrc.ec.europa.eu/content/lucas-2009-topsoil-data with details of the larger European Soil Data Centre project at http://doi.org/10.17616/R34069. Access to model code is currently restricted to those directly collaborating with the MEMS development team. This is to ensure all bugs are caught and treated before release to the public. Detailed information and code relevant to specific questions can be provided upon request.

Supplementary materials

See separate attachments

Author Contribution

All authors contributed to the conceptualization of the MEMS model framework with MFC, KP and MDW formalizing the original foundational science. The *in-practice* model structure was then formalized by ADR, MFC, KP, SO and MWD. All model building, coding, statistical analyses and data analysis on the measured fractionation data and all model-measure comparisons was performed by ADR. Guidance on the optimisation procedures was provided by SO. The LUCAS database was provided by EL and all initial analysis and preparation of the data (e.g., refining bulk density estimates and NPP values for each site) was performed by EL. The project was overseen by all authors but primarily led by MFC. Funding was initially provided by MDW and later through grants awarded to MFC and KP. Developing, testing and evaluating the model was performed solely by ADR, as was all data presentation apart from the final conceptual diagram (Figure 1) which was outsourced (see acknowledgments). The manuscript was written and edited by ADR with comments and feedback from all co-authors.

Competing Interests

The authors declare that they have no conflict of interest.

Acknowledgments

This research was supported by a National Science Foundation CAREER grant (number 255228) awarded to MDW, the US DOE Advanced Research Projects Agency-Energy program (ROOTS project; DE-FOA-00001565), the NSF-DEB Award #1743237 and the JRC (purchase order D.B720517). The authors like to thank Michelle Haddix for the soil organic matter fractionation work and Dr. Yao Zhang for help with regards to various parts of data generation (e.g., climate inputs) and model development. The conceptual figure diagram was redrawn and stylized by Katie Burnet.

References

Aber, J. D., Melillo, J. M., & McClaugherty, C. A. (1990). Predicting long-term patterns of mass loss, nitrogen dynamics, and soil organic matter formation from initial fine litter chemistry in temperate forest ecosystems. *Canadian Journal of Botany*, 68(10), 2201-2208.

Abramoff, R., Xu, X., Hartman, M., O'Brien, S., Feng, W., Davidson, E., Finzi, A., Moorhead, D., Schimel, J., Torn, M. & Mayes, M. A. (2018). The Millennial model: in search of measurable pools and transformations for modeling soil carbon in the new century. *Biogeochemistry*, 137(1-2), 51-71.

Ahrens, B., Braakhekke, M. C., Guggenberger, G., Schrumpf, M., & Reichstein, M. (2015). Contribution of sorption, DOC transport and microbial interactions to the 14C age of a soil organic carbon profile: Insights from a calibrated process model. *Soil Biology and Biochemistry*, 88, 390-402.

Allison, S. D. (2012). A trait-based approach for modelling microbial litter decomposition. *Ecology letters*, 15(9), 1058-1070.

Allison, S. D., Wallenstein, M. D., & Bradford, M. A. (2010). Soil-carbon response to warming dependent on microbial physiology. *Nature Geoscience*, 3(5), 336.

Arora, V. K., Boer, G. J., Friedlingstein, P., Eby, M., Jones, C. D., Christian, J. R., Bonan, G., Bopp, L., Brovkin, V., Cadule, P., Hajima, T., Ilyini, T., Lindsay, K., Tjiputra, J.F. & Wu, T. (2013). Carbon–concentration and carbon–climate feedbacks in CMIP5 Earth system models. *Journal of Climate*, 26(15), 5289-5314.

Averill, C., & Waring, B. (2018). Nitrogen limitation of decomposition and decay: How can it occur?. *Global Change Biology*, 24(4), 1417-1427.

Beare, M. H., McNeill, S. J., Curtin, D., Parfitt, R. L., Jones, H. S., Dodd, M. B., & Sharp, J. (2014). Estimating the organic carbon stabilisation capacity and saturation deficit of soils: a New Zealand case study. *Biogeochemistry*, 120(1-3), 71-87.

Berg, B. (2000). Litter decomposition and organic matter turnover in northern forest soils. *Forest ecology and Management*, 133(1-2), 13-22.

Braakhekke, M. C., Beer, C., Hoosbeek, M. R., Reichstein, M., Kruijt, B., Schrumpf, M., & Kabat, P. (2011). SOMPROF: A vertically explicit soil organic matter model. *Ecological modelling*, 222(10), 1712-1730.

Bradford, M. A., Watts, B. W., & Davies, C. A. (2010). Thermal adaptation of heterotrophic soil respiration in laboratory microcosms. *Global Change Biology*, 16(5), 1576-1588.

Bu, R., Lu, J., Ren, T., Liu, B., Li, X., & Cong, R. (2015). Particulate organic matter affects soil nitrogen mineralization under two crop rotation systems. *PLoS One*, 10(12), e0143835.

Büks, F., & Kaupenjohann, M. (2016). Enzymatic biofilm digestion in soil aggregates facilitates the release of particulate organic matter by sonication. *Soil*, 2(4), 499-509.

Cambardella, C. A., & Elliott, E. T. (1992). Particulate soil organic-matter changes across a grassland cultivation sequence. *Soil science society of America journal*, 56(3), 777-783.

Campbell, E. E., & Paustian, K. (2015). Current developments in soil organic matter modeling and the expansion of model applications: a review. *Environmental Research Letters*, 10(12), 123004.

Campbell, E. E., Parton, W. J., Soong, J. L., Paustian, K., Hobbs, N. T., & Cotrufo, M. F. (2016). Using litter chemistry controls on microbial processes to partition litter carbon fluxes with the litter decomposition and leaching (LIDEL) model. *Soil Biology and Biochemistry*, 100, 160-174.

Canadell, J., Jackson, R. B., Ehleringer, J. B., Mooney, H. A., Sala, O. E., & Schulze, E. D. (1996). Maximum rooting depth of vegetation types at the global scale. *Oecologia*, 108(4), 583-595.

Carrington, E. M., Hernes, P. J., Dyda, R. Y., Plante, A. F., & Six, J. (2012). Biochemical changes across a carbon saturation gradient: lignin, cutin, and suberin decomposition and stabilization in fractionated carbon pools. *Soil Biology and Biochemistry*, 47, 179-190.

Castellano, M. J., Mueller, K. E., Olk, D. C., Sawyer, J. E., & Six, J. (2015). Integrating plant litter quality, soil organic matter stabilization, and the carbon saturation concept. *Global Change Biology*, 21(9), 3200-3209.

Christensen, B. T. (1992). Physical fractionation of soil and organic matter in primary particle size and density separates. In Advances in soil science (pp. 1-90). Springer, New York, NY.

Cotrufo, M. F., Soong, J. L., Horton, A. J., Campbell, E. E., Haddix, M. L., Wall, D. H., & Parton, W. J. (2015). Formation of soil organic matter via biochemical and physical pathways of litter mass loss. *Nature Geoscience*, 8(10), ngeo2520.

Cotrufo, M. F., Wallenstein, M. D., Boot, C. M., Denef, K., & Paul, E. (2013). The M icrobial E fficiency-M atrix S tabilization (MEMS) framework integrates plant litter decomposition with soil organic matter stabilization: do labile plant inputs form stable soil organic matter?. *Global Change Biology*, 19(4), 988-995.

Cotrufo, M.F., Ranalli, M.G., Haddix, M.L., Six, J. and Lugato, E., (2018). Drivers of soil C:N stoichiometry and implication for soil carbon accrual. *Science*, in review

Crow, S. E., Swanston, C. W., Lajtha, K., Brooks, J. R., & Keirstead, H. (2007). Density fractionation of forest soils: methodological questions and interpretation of incubation results and turnover time in an ecosystem context. *Biogeochemistry*, 85(1), 69-90.

DeGryze, S., Six, J., Paustian, K., Morris, S. J., Paul, E. A., & Merckx, R. (2004). Soil organic carbon pool changes following land-use conversions. *Global Change Biology*, 10(7), 1120-1132.

Dorodnikov, M., Blagodatskaya, E., Blagodatsky, S., Marhan, S., Fangmeier, A., & Kuzyakov, Y. (2009). Stimulation of microbial extracellular enzyme activities by elevated CO2 depends on soil aggregate size. *Global Change Biology*, 15(6), 1603-1614.

Dungait, J. A., Hopkins, D. W., Gregory, A. S., & Whitmore, A. P. (2012). Soil organic matter turnover is governed by accessibility not recalcitrance. *Global Change Biology*, 18(6), 1781-1796.

Dwivedi, D., Riley, W. J., Torn, M. S., Spycher, N., Maggi, F., & Tang, J. Y. (2017). Mineral properties, microbes, transport, and plant-input profiles control vertical distribution and age of soil carbon stocks. *Soil Biology and Biochemistry*, 107, 244-259.

Elliott, E. T., Paustian, K., & Frey, S. D. (1996). Modeling the measurable or measuring the modelable: A hierarchical approach to isolating meaningful soil organic matter fractionations. In Evaluation of soil organic matter models (pp. 161-179). Springer, Berlin, Heidelberg.

Feng, W. (2012). Testing the soil carbon saturation theory: maximal carbon stabilization and soil organic matter stability as a function of organic carbon inputs. PhD Thesis, University of Pennsylvania

Filley, T. R., Boutton, T. W., Liao, J. D., Jastrow, J. D., & Gamblin, D. E. (2008). Chemical changes to nonaggregated particulate soil organic matter following grassland-to-woodland transition in a subtropical savanna. *Journal of Geophysical Research: Biogeosciences*, 113(G3).

Frouz, J. (2018). Effects of soil macro-and mesofauna on litter decomposition and soil organic matter stabilization. *Geoderma*, 332, 161-172.

Gentile, R., Vanlauwe, B., & Six, J. (2011). Litter quality impacts short-but not long-term soil carbon dynamics in soil aggregate fractions. *Ecological Applications*, 21(3), 695-703.

Gulde, S., Chung, H., Amelung, W., Chang, C., & Six, J. (2008). Soil carbon saturation controls labile and stable carbon pool dynamics. *Soil Science Society of America Journal*, 72(3), 605-612.

Haddix, M. L., Paul, E. A., & Cotrufo, M. F. (2016). Dual, differential isotope labeling shows the preferential movement of labile plant constituents into mineral-bonded soil organic matter. *Global Change Biology*, 22(6), 2301-2312.

Harmon, M., and J. Domingo (2001), A User's Guide to STANDCARB Version 2.0: A Model to Simulate the Carbon Stores in Forest Stands, Dep. of For. Sci., Oreg. State Univ., Corvallis.

Heckman, K., Grandy, A. S., Gao, X., Keiluweit, M., Wickings, K., Carpenter, K., Chorover, J. & Rasmussen, C. (2013). Sorptive fractionation of organic matter and formation of organo-hydroxy-aluminum complexes during litter biodegradation in the presence of gibbsite. *Geochimica et Cosmochimica Acta*, 121, 667-683.

Huang, P. M., Wang, M. K., & Chiu, C. Y. (2005). Soil mineral–organic matter–microbe interactions: impacts on biogeochemical processes and biodiversity in soils. *Pedobiologia*, 49(6), 609-635.

Jackson, R. B., Canadell, J., Ehleringer, J. R., Mooney, H. A., Sala, O. E., & Schulze, E. D. (1996). A global analysis of root distributions for terrestrial biomes. *Oecologia*, 108(3), 389-411.

Jenkinson, D. S. (1977). Studies on the decomposition of plant material in soil. V. The effects of plant cover and soil type on the loss of carbon from14c labelled ryegrass decomposing under field conditions. *Journal of Soil Science*, 28(3), 424-434.

Jenkinson, D. S., & Rayner, J. H. (1977). The turnover of soil organic matter in some of the Rothamsted classical experiments. *Soil science*, 123(5), 298-305.

Jilling, A., Keiluweit, M., Contosta, A. R., Frey, S., Schimel, J., Schnecker, J., Smith, R. G., Tieman, L. & Grandy, A. S. Minerals in the rhizosphere: overlooked mediators of soil nitrogen availability to plants and microbes. *Biogeochemistry*, 1-20.

Jones, C., & Falloon, P. (2009). Sources of uncertainty in global modelling of future soil organic carbon storage. In Uncertainties in Environmental Modelling and Consequences for Policy Making (pp. 283-315). Springer, Dordrecht.

Kalbitz, K., Schwesig, D., Rethemeyer, J., & Matzner, E. (2005). Stabilization of dissolved organic matter by sorption to the mineral soil. *Soil Biology and Biochemistry*, 37(7), 1319-1331.

Kallenbach, C. M., Frey, S. D., & Grandy, A. S. (2016). Direct evidence for microbial-derived soil organic matter formation and its ecophysiological controls. *Nature communications*, 7, 13630.

Kindler, R., Siemens, J. A. N., Kaiser, K., Walmsley, D. C., Bernhofer, C., Buchmann, N., ... & Heim, A. (2011). Dissolved carbon leaching from soil is a crucial component of the net ecosystem carbon balance. *Global Change Biology*, 17(2), 1167-1185.

Kleber, M., Nico, P. S., Plante, A., Filley, T., Kramer, M., Swanston, C., & Sollins, P. (2011). Old and stable soil organic matter is not necessarily chemically recalcitrant: implications for modeling concepts and temperature sensitivity. *Global Change Biology*, 17(2), 1097-1107.

Klotzbücher, T., Kaiser, K., Guggenberger, G., Gatzek, C., & Kalbitz, K. (2011). A new conceptual model for the fate of lignin in decomposing plant litter. *Ecology*, 92(5), 1052-1062.

Kögel-Knabner, I., Guggenberger, G., Kleber, M., Kandeler, E., Kalbitz, K., Scheu, S., Eusterhues, K. & Leinweber, P. (2008). Organo-mineral associations in temperate soils: Integrating biology, mineralogy, and organic matter chemistry. *Journal of Plant Nutrition and Soil Science*, 171(1), 61-82.

Kolka, R., Weishampel, P., & Fröberg, M. (2008). Measurement and importance of dissolved organic carbon. In Field measurements for forest carbon monitoring (pp. 171-176). Springer, Dordrecht.

Kothawala, D. N., Moore, T. R., & Hendershot, W. H. (2008). Adsorption of dissolved organic carbon to mineral soils: A comparison of four isotherm approaches. *Geoderma*, 148(1), 43-50.

Kothawala, D. N., Moore, T. R., & Hendershot, W. H. (2009). Soil properties controlling the adsorption of dissolved organic carbon to mineral soils. *Soil Science Society of America Journal*, 73(6), 1831-1842.

Kothawala, D. N., Roehm, C., Blodau, C., & Moore, T. R. (2012). Selective adsorption of dissolved organic matter to mineral soils. *Geoderma*, 189, 334-342.

Kuhn, M., & Johnson, K. (2013). Applied predictive modeling (Vol. 26). New York: Springer.

Kuzyakov, Y. (2010). Priming effects: interactions between living and dead organic matter. *Soil Biology and Biochemistry*, 42(9), 1363-1371.

Lawrence, C. R., Neff, J. C., & Schimel, J. P. (2009). Does adding microbial mechanisms of decomposition improve soil organic matter models? A comparison of four models using data from a pulsed rewetting experiment. *Soil Biology and Biochemistry*, 41(9), 1923-1934.

Lehmann, J., & Kleber, M. (2015). The contentious nature of soil organic matter. *Nature*, 528(7580), 60.

Li, C., Frolking, S., & Frolking, T. A. (1992). A model of nitrous oxide evolution from soil driven by rainfall events: 1. Model structure and sensitivity. *Journal of Geophysical Research: Atmospheres*, 97(D9), 9759-9776.

Liang, C., Schimel, J. P., & Jastrow, J. D. (2017). The importance of anabolism in microbial control over soil carbon storage. *Nature microbiology*, 2(8), 17105.

Ludwig, M., Achtenhagen, J., Miltner, A., Eckhardt, K. U., Leinweber, P., Emmerling, C., & Thiele-Bruhn, S. (2015). Microbial contribution to SOM quantity and quality in density fractions of temperate arable soils. *Soil Biology and Biochemistry*, *81*, 311-322.

Luo, Y., Ahlström, A., Allison, S. D., Batjes, N. H., Brovkin, V., Carvalhais, N., ... & Georgiou, K. (2016). Toward more realistic projections of soil carbon dynamics by Earth system models. *Global Biogeochemical Cycles*, 30(1), 40-56.

Lützow, M. V., Kögel-Knabner, I., Ekschmitt, K., Matzner, E., Guggenberger, G., Marschner, B., & Flessa, H. (2006). Stabilization of organic matter in temperate soils: mechanisms and their relevance under different soil conditions–a review. *European Journal of Soil Science*, 57(4), 426-445.

Malamoud, K., McBratney, A. B., Minasny, B., & Field, D. J. (2009). Modelling how carbon affects soil structure. *Geoderma*, 149(1-2), 19-26.

Manzoni, S., Jackson, R. B., Trofymow, J. A., & Porporato, A. (2008). The global stoichiometry of litter nitrogen mineralization. Science, 321(5889), 684-686.

Manzoni, S., Moyano, F., Kätterer, T., & Schimel, J. (2016). Modeling coupled enzymatic and solute transport controls on decomposition in drying soils. *Soil Biology and Biochemistry*, 95, 275-287.

Marschner, B., Brodowski, S., Dreves, A., Gleixner, G., Gude, A., Grootes, P. M., ... & Kaiser, K. (2008). How relevant is recalcitrance for the stabilization of organic matter in soils?. *Journal of plant nutrition and soil science*, 171(1), 91-110.

Mayes, M. A., Heal, K. R., Brandt, C. C., Phillips, J. R., & Jardine, P. M. (2012). Relation between soil order and sorption of dissolved organic carbon in temperate subsoils. *Soil Science Society of America Journal*, 76(3), 1027-1037.

McGill, W.B., and C.V. Cole (1981) Comparative aspects of cycling of organic C, N, S and P through soil organic matter. *Geoderma* 26:267-286.

Miki, T., Ushio, M., Fukui, S., & Kondoh, M. (2010). Functional diversity of microbial decomposers facilitates plant coexistence in a plant–microbe–soil feedback model. *Proceedings of the National Academy of Sciences*, 107(32), 14251-14256.

Mikutta, R., Kleber, M., Torn, M. S., & Jahn, R. (2006). Stabilization of soil organic matter: association with minerals or chemical recalcitrance? *Biogeochemistry*, 77(1), 25-56.

Moorhead, D. L., Lashermes, G., Sinsabaugh, R. L., & Weintraub, M. N. (2013). Calculating co-metabolic costs of lignin decay and their impacts on carbon use efficiency. *Soil Biology and Biochemistry*, 66, 17-19.

Moorhead, D., Lashermes, G., Recous, S., & Bertrand, I. (2014). Interacting microbe and litter quality controls on litter decomposition: a modeling analysis. *PloS one*, 9(9), e108769.

NOAA (2018) CPC Global Temperature data provided by the NOAA/OAR/ESRL PSD, Boulder, Colorado, USA, from their Web site at https://www.esrl.noaa.gov/psd/

ORNL DAAC (2009) MODIS and VIIRS Land Products Global Subsetting and Visualization Tool. ORNL DAAC, Oak Ridge, Tennessee, USA. Accessed March 20, 2016. Subset obtained for MOD13Q1 product at various sites in Spatial Range: N=70.00N, S=20.00N, E=35.00, W=-15.00W, time period: 2009 to 2009, and subset size: 0.25 x 0.25 km.

852 Parton, W. J., Schimel, D. S., Cole, C. V., & Ojima, D. S. (1987). Analysis of factors controlling soil organic matter
853 levels in Great Plains Grasslands 1. *Soil Science Society of America Journal*, 51(5), 1173-1179.
854 Paton, T., Humphreys, G.S., Mitchell, P., 1995. Soils: A New Global View. Yale Univ. Press, New Haven [u.a.],
855 pp.33–67 (Chapter3.Bioturbation).
856 Paul, E. A. & van Veen, J. A. (1978). The use of tracers to determine the dynamic nature of organic matter. *Trans.*
857 *11th Int. Congress of Soil Science*, 3, 61-102.
858 Poeplau, C. (2016). Estimating root: shoot ratio and soil carbon inputs in temperate grasslands with the RothC model.
859 *Plant and soil*, 407(1-2), 293-305.
860 Poeplau, C., & Don, A. (2013). Sensitivity of soil organic carbon stocks and fractions to different land-use changes
861 across Europe. *Geoderma*, 192, 189-201.
862 Poeplau, C., Don, A., Six, J., Kaiser, M., Benbi, D., Chenu, C., ... & Gregorich, E. (2018). Isolating organic carbon
863 fractions with varying turnover rates in temperate agricultural soils–A comprehensive method comparison. *Soil*
864 *Biology and Biochemistry*, 125, 10-26.
865 Poeplau, C., Kätterer, T., Leblans, N. I., & Sigurdsson, B. D. (2017). Sensitivity of soil carbon fractions and their
866 specific stabilization mechanisms to extreme soil warming in a subarctic grassland. *Global Change Biology*,
867 23(3), 1316-1327.
868 R Core Team (2018). R: A language and environment for statistical computing. R Foundation for Statistical
869 Computing, Vienna, Austria. URL https://www.R-project.org/.
870 Saltelli, A., Ratto, M., Andres, T., Campolongo, F., Cariboni, J., Gatelli, D., ... & Tarantola, S. (2008). Global
871 sensitivity analysis: the primer. John Wiley & Sons.
872 Scheibe, A., & Gleixner, G. (2014). Influence of litter diversity on dissolved organic matter release and soil carbon
873 formation in a mixed beech forest. *PloS one*, 9(12), e114040.
874 Scheu, S., & Wolters, V. (1991). Influence of fragmentation and bioturbation on the decomposition of 14C-labelled
875 beech leaf litter. *Soil Biology and Biochemistry*, 23(11), 1029-1034.
876 Schmidt, M. W., Torn, M. S., Abiven, S., Dittmar, T., Guggenberger, G., Janssens, I. A., ... & Nannipieri, P. (2011).
877 Persistence of soil organic matter as an ecosystem property. *Nature*, 478(7367), 49.
878 Setia, R., Verma, S. L., & Marschner, P. (2012). Measuring microbial biomass carbon by direct extraction–
879 comparison with chloroform fumigation-extraction. *European journal of soil biology*, 53, 103-106.
880 Sierra, C. A., Malghani, S., & Müller, M. (2015). Model structure and parameter identification of soil organic matter
881 models. *Soil Biology and Biochemistry*, 90, 197-203.
882 Sima, N. Q., Harmel, R. D., Fang, Q. X., Ma, L., & Andales, A. A. (2018). A modified F-test for evaluating model
883 performance by including both experimental and simulation uncertainties. *Environmental Modelling &*
884 *Software*, 104, 236-248.
885 Sinsabaugh, R. L., Manzoni, S., Moorhead, D. L., & Richter, A. (2013). Carbon use efficiency of microbial
886 communities: stoichiometry, methodology and modelling. *Ecology letters*, 16(7), 930-939.
887 Six, J., Conant, R. T., Paul, E. A., & Paustian, K. (2002). Stabilization mechanisms of soil organic matter: implications
888 for C-saturation of soils. *Plant and soil*, 241(2), 155-176.
889 Smith, P., Smith, J. U., Powlson, D. S., McGill, W. B., Arah, J. R. M., Chertov, O. G., ... & Jensen, L. S. (1997). A
890 comparison of the performance of nine soil organic matter models using datasets from seven long-term
891 experiments. *Geoderma*, 81(1-2), 153-225.
892 Sobol, I. M. (2001). Global sensitivity indices for nonlinear mathematical models and their Monte Carlo estimates.
893 *Mathematics and computers in simulation*, 55(1-3), 271-280.
894 Soetaert, K., Petzoldt, T., & Setzer, R. W. (2010). Solving Differential Equations in R: Package deSolve. *Journal of*
895 *Statistical Software*, 33(9), 1—25
896 Soong, J. L., Parton, W. J., Calderon, F., Campbell, E. E., & Cotrufo, M. F. (2015). A new conceptual model on the
897 fate and controls of fresh and pyrolized plant litter decomposition. *Biogeochemistry*, 124(1-3), 27-44.
898 Soong, J. L., Vandegehuchte, M. L., Horton, A. J., Nielsen, U. N., Denef, K., Shaw, E. A., de Tomasel, C. M., Parton,
899 W., Wall, D. H. & Cotrufo, M. F. (2016). Soil microarthropods support ecosystem productivity and soil C
900 accrual: evidence from a litter decomposition study in the tallgrass prairie. *Soil Biology and Biochemistry*, *92*,
901 230-238.
902 Stewart, C. E., Paustian, K., Conant, R. T., Plante, A. F., & Six, J. (2007). Soil carbon saturation: concept, evidence
903 and evaluation. *Biogeochemistry*, 86(1), 19-31.
904 Stewart, C. E., Plante, A. F., Paustian, K., Conant, R. T., & Six, J. (2008). Soil Carbon Saturation: Linking Concept
905 and Measurable Carbon Pools. *Soil Science Society of America Journal*, 72(2), 379-392.
906 Stockmann, U., Adams, M. A., Crawford, J. W., Field, D. J., Henakaarchchi, N., Jenkins, M., ... & Wheeler, I. (2013).
907 The knowns, known unknowns and unknowns of sequestration of soil organic carbon. *Agriculture, Ecosystems*
908 *& Environment*, 164, 80-99.
909 Stout, J. D. & O'Brien, B. J. (1973). Factors affecting radiocarbon enrichment in soil and the turnover of soil organic
910 matter. Proceedings of the 8th International Conference on Radiocarbon Dating, Vol. 2, pp. 394-407,
911 Wellington, New Zealand.

Subke, J. A., Inglima, I., & Francesca Cotrufo, M. (2006). Trends and methodological impacts in soil CO2 efflux partitioning: a metaanalytical review. *Global Change Biology*, 12(6), 921-943.

Swift, M. J., Heal, O. W., Anderson, J. M., & Anderson, J. M. (1979). Decomposition in terrestrial ecosystems (Vol. 5). Univ of California Press.

Tan, Z., Lal, R., Owens, L., & Izaurralde, R. C. (2007). Distribution of light and heavy fractions of soil organic carbon as related to land use and tillage practice. *Soil and Tillage Research*, 92(1-2), 53-59.

Tappi (1981) Water solubility of wood and pulp. Test method T204 (or 207). Technical Association of the Pulp and Paper Industry, Atlanta

Toth G., Jones A., Montanarella L. (2013) LUCAS Topsoil Survey — methodology, data and results. In: JRC Technical Reports. European Union, Luxemburg.

Treseder, K. K., Balser, T. C., Bradford, M. A., Brodie, E. L., Dubinsky, E. A., Eviner, V. T., ... & Pett-Ridge, J. (2012). Integrating microbial ecology into ecosystem models: challenges and priorities. *Biogeochemistry*, 109(1-3), 7-18.

Trumbore, S. E., Schiff, S. L., Aravena, R., & Elgood, R. (1992). Sources and transformation of dissolved organic carbon in the Harp Lake forested catchment: the role of soils. *Radiocarbon*, 34(3), 626-635.

Van Soest PJ, Robertson JB, Lewis BA (1991) Methods for dietary fiber, neutral detergent fiber, and nonstarch polysaccharides in relation to animal nutrition. *Journal of Dairy Science*, 74(10):3583–3597.

Van Soest PJ, Wine RH (1968) Determination of lignin and cellulose in acid-detergent fiber with permanganate. *Journal of Associated Official Analytical Chemistry*, 51(4):780

Větrovský, T., Steffen, K. T., & Baldrian, P. (2014). Potential of cometabolic transformation of polysaccharides and lignin in lignocellulose by soil Actinobacteria. *PLoS One*, 9(2), e89108.

von Lützow, M., Kögel-Knabner, I., Ekschmitt, K., Flessa, H., Guggenberger, G., Matzner, E., & Marschner, B. (2007). SOM fractionation methods: relevance to functional pools and to stabilization mechanisms. *Soil Biology and Biochemistry*, 39(9), 2183-2207.

Wallenstein, M. D., & Hall, E. K. (2012). A trait-based framework for predicting when and where microbial adaptation to climate change will affect ecosystem functioning. *Biogeochemistry*, 109(1-3), 35-47.

Wander, M. (2004). Soil organic matter fractions and their relevance to soil function. Soil organic matter in sustainable agriculture. CRC Press, Boca Raton, FL, 67-102.

Wang, G., Post, W. M., & Mayes, M. A. (2013). Development of microbial-enzyme-mediated decomposition model parameters through steady-state and dynamic analyses. *Ecological Applications*, 23(1), 255-272.

Waring, B. G., Averill, C., & Hawkes, C. V. (2013). Differences in fungal and bacterial physiology alter soil carbon and nitrogen cycling: insights from meta-analysis and theoretical models. *Ecology letters*, 16(7), 887-894.

Wieder, W. R., Allison, S. D., Davidson, E. A., Georgiou, K., Hararuk, O., He, Y., ... & Todd-Brown, K. (2015). Explicitly representing soil microbial processes in Earth system models. *Global Biogeochemical Cycles*, 29(10), 1782-1800.

Wieder, W. R., Bonan, G. B., & Allison, S. D. (2013). Global soil carbon projections are improved by modelling microbial processes. *Nature Climate Change*, 3(10), 909.

Wieder, W. R., Grandy, A. S., Kallenbach, C. M., & Bonan, G. B. (2014). Integrating microbial physiology and physio-chemical principles in soils with the MIcrobial-MIneral Carbon Stabilization (MIMICS) model. *Biogeosciences*, 11(14), 3899-3917.

Williams, J. R., Jones, C. A., & Dyke, P. T. (1984). A modeling approach to determining the relationship between erosion and soil productivity. *Transactions of the ASAE*, 27(1), 129-0144.

Xu, X., Schimel, J. P., Thornton, P. E., Song, X., Yuan, F., & Goswami, S. (2014). Substrate and environmental controls on microbial assimilation of soil organic carbon: a framework for Earth system models. *Ecology Letters*, 17(5), 547-555.

Yoo, K., Ji, J., Aufdenkampe, A., & Klaminder, J. (2011). Rates of soil mixing and associated carbon fluxes in a forest versus tilled agricultural field: Implications for modeling the soil carbon cycle. Journal of Geophysical Research: *Biogeosciences*, 116(G1).

Zimmermann, M., Leifeld, J., Schmidt, M. W. I., Smith, P., & Fuhrer, J. (2007). Measured soil organic matter fractions can be related to pools in the RothC model. *European Journal of Soil Science*, 58(3), 658-667.

Biogeosciences Discuss., https://doi.org/10.5194/bg-2018-430
Manuscript under review for journal Biogeosciences
Discussion started: 17 October 2018

964 **Figures**

965 **Figure 1 - Conceptual model diagram of MEMS v1.0 (see Table 1 for detailed information regarding each pool). Litter**
966 **pools of MEMS v1.0 are defined as > 2mm particles and comprise of hot-water extractable (C1), acid-soluble (C2) and acid-**
967 **insoluble (C3) fractions. A microbial pool (C4) and dissolved carbon pool (C6) are also part of the organic horizon and**
968 **litter decomposition processes (see LIDEL for more information, Campbell et al., 2016). Soil organic matter (< 2mm**
969 **particles belowground) comprises of a light particulate organic matter pool (light POM, C10) formed from the input**
970 **through fragmentation and physical transfer of the structural litter residues (C2 and C3), a coarse heavy POM pool (C5)**
971 **formed from both litter fragmentation and microbial residues coating sand-sized particles, a dissolved organic matter**
972 **(DOM) pool (C8) formed from the decomposition of all other pools and receiving DOM from the organic soil layer, and a**
973 **mineral-associated organic matter pool (MAOM C9), which exchanges C through sorption and desorption with the DOM.**
974 **Arrows indicate the fluxes of carbon between the different pools. Carbon dioxide is produced from a number of these fluxes**
975 **but for simplicity of graphical representation, these arrows are not linked to the carbon dioxide pool (C7). Deeper soil**
976 **layers can be represented by the same structure, with or without root inputs depending on depth, but are not implemented**
977 **in this inaugural version of MEMS v1.0.**

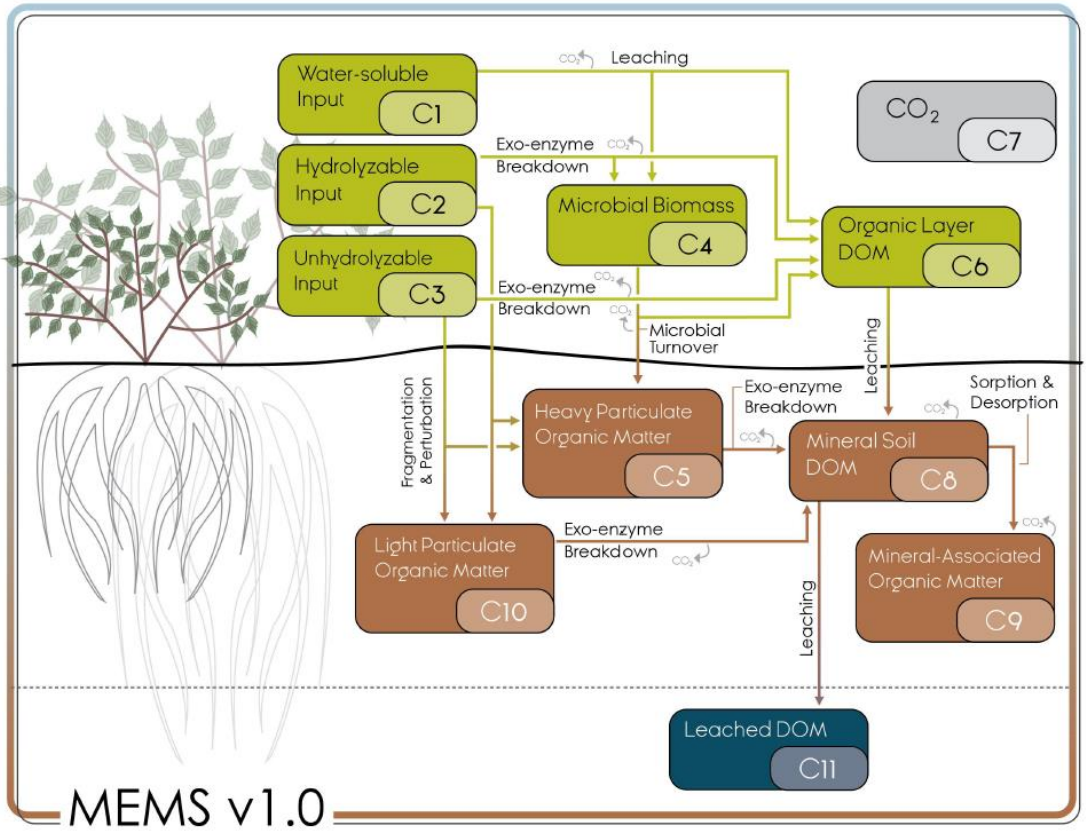

978
979

Biogeosciences Discuss., https://doi.org/10.5194/bg-2018-430
Manuscript under review for journal Biogeosciences
Discussion started: 17 October 2018

Figure 2 - Global sensitivity analysis results showing the relative contribution of each parameter to a change in carbon stock of each pool in MEMS v1.0 (leached carbon to deeper soil layers [pool C11] is omitted for clarity). Details of each parameter and the abbreviations used can be found in Table 2. The sensitivity analysis was repeated annually for simulation times between 1 and 100 years, every 10 years after that to 400-year simulations and every 100 years after that up to a 1000-year simulation. Results are presented on a log scale in years. Parameters involved in different SOM formation processes are grouped by colour: yellows – parameters that define DOM leaching from the organic horizon to the soil layer; reds – parameters that affect microbial carbon use efficiency, purples – parameters that affect organic matter vertical transport to deeper layers, greens – maximum decay rates.

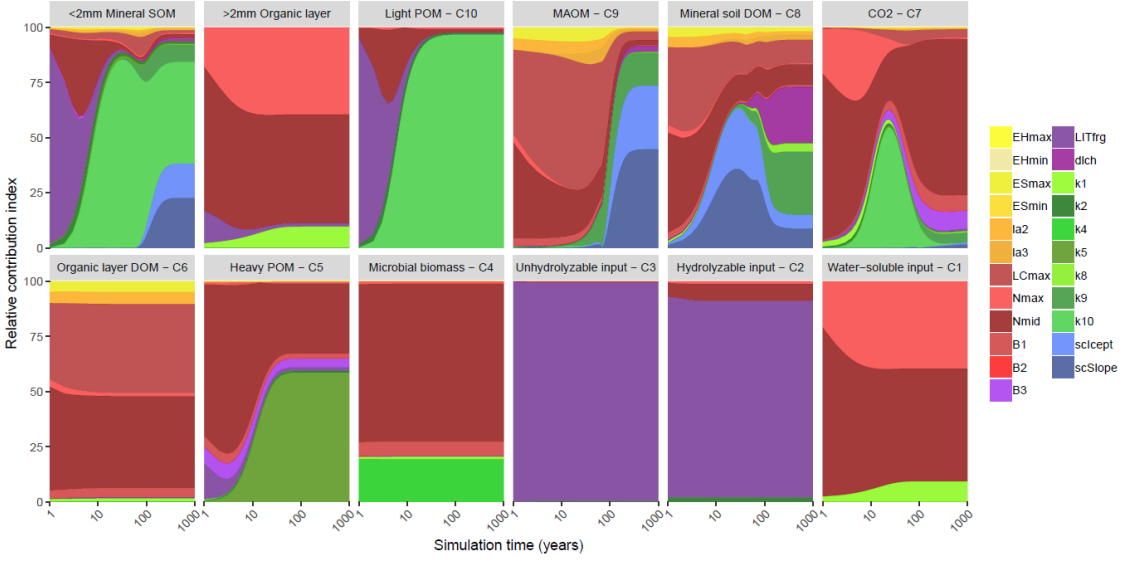

Biogeosciences Discuss., https://doi.org/10.5194/bg-2018-430
Manuscript under review for journal Biogeosciences
Discussion started: 17 October 2018

Figure 3 - The ratio between mineral-associated organic matter and total particulate organic matter (MAOM:POM) under steady-state input conditions in MEMS v1.0 as a response to the full, realistic range of driving variables. Note, total POM refers to the sum of pools C5 and C10. Each input was varied individually while all others remained fixed at baseline values (indicated by dashed lines) – mean, maximum and minimum values for litter chemistry driving variables (*LitN*, *fDOC*, *fLIG* and *fSOL*) were derived from Campbell *et al.* (2016) and edaphic, climatic and C input driving variables (soil bulk density, sand content, soil pH, mean annual temperature and annual net primary productivity) were derived from the LUCAS dataset (Toth *et al.*, 2013).

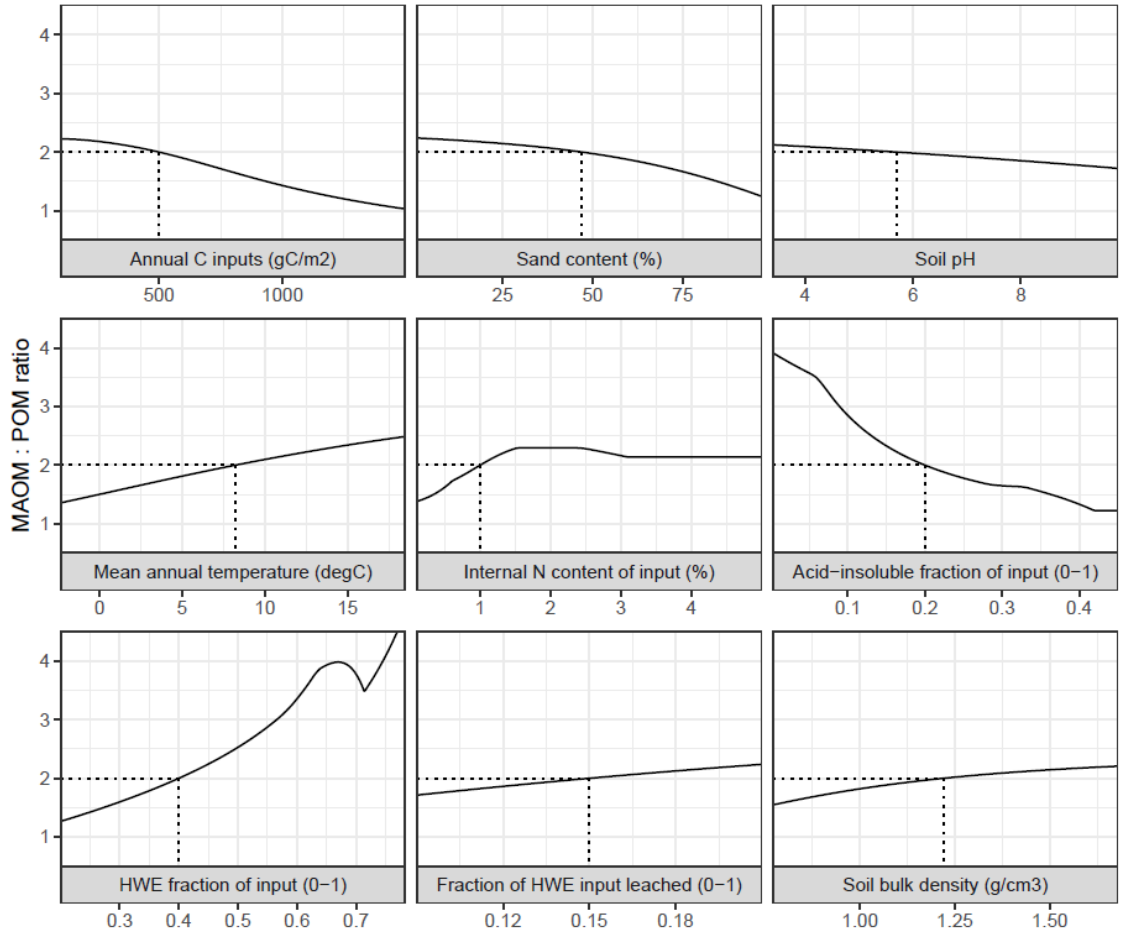

Biogeosciences Discuss., https://doi.org/10.5194/bg-2018-430
Manuscript under review for journal Biogeosciences
Discussion started: 17 October 2018

Figure 4 - Mineral-associated organic matter (MAOM) stock response to different levels of input litter quality and quantity, compared for edaphic conditions which equate to different MAOM sorption relationships in MEMS v1.0. Formatting adopted from Castellano *et al.* (2015) to aid comparison between the hypothetical relationship postulated and the actual response simulated by MEMS v1.0 here.

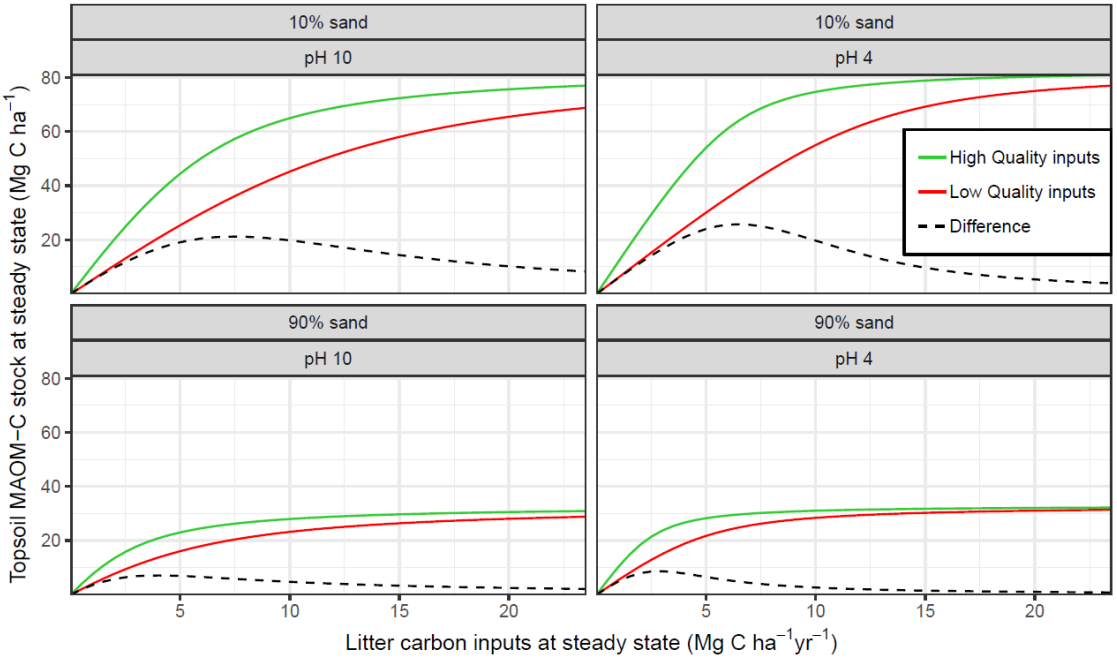

Biogeosciences Discuss., https://doi.org/10.5194/bg-2018-430
Manuscript under review for journal Biogeosciences
Discussion started: 17 October 2018

Figure 5 - Measured and modelled soil C stocks (split into mineral-associated organic matter, MAOM, total particulate organic matter, POM, and total soil organic carbon, SOC) for the forest and grassland land-use classes of the fractionated sites from the LUCAS dataset (*n* = 154). Note that the MAOM:POM ratio facet is unitless, not as shown by the y-axis label. Also note the free y-axis scales and that total POM is a sum of both light and heavy fractions.

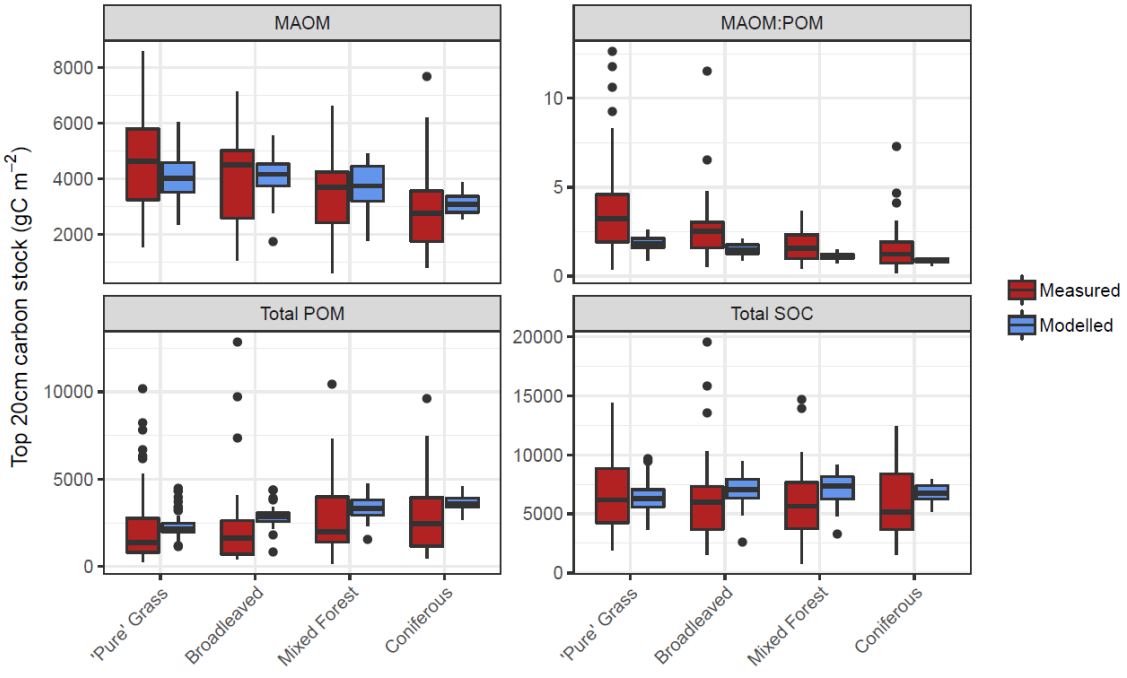

Biogeosciences Discuss., https://doi.org/10.5194/bg-2018-430
Manuscript under review for journal Biogeosciences
Discussion started: 17 October 2018

Figure 6 - Comparisons between average (± 1 standard error) measured (red) and modelled (blue) bulk SOC stocks for 8192 forestry and grassland sites over a climatic and edaphic gradient across Europe. Each comparison is partitioned into high and low groups of mean annual precipitation, MAP (top *vs* bottom panels), mean annual temperature, MAT (left *vs* right panels) and soil texture (alternating panels left to right). ANOVA comparisons of means is performed to show significant differences (* p < 0.001, ** p < 0.01, * p < 0.05). Number of samples for each land use and division is shown at the base of each bar.**

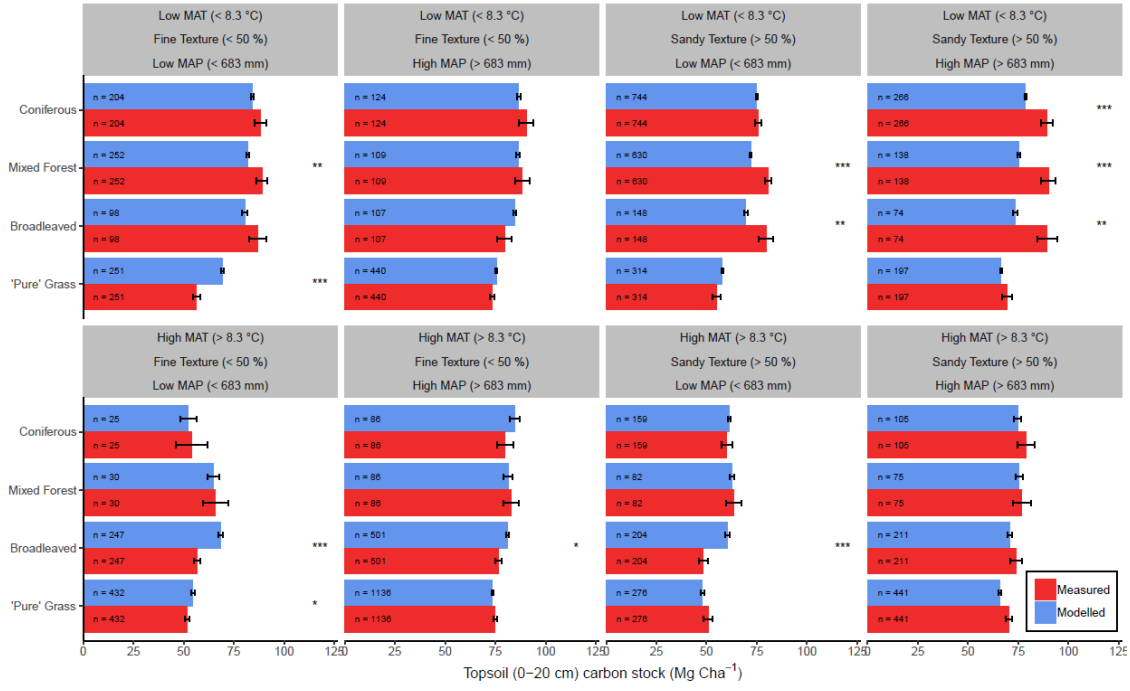

Biogeosciences Discuss., https://doi.org/10.5194/bg-2018-430
Manuscript under review for journal Biogeosciences
Discussion started: 17 October 2018

Figure 7 - Model residuals of topsoil (0-20 cm) C stocks (Mg C ha^{-1}) for 8192 sites (3487 grasslands, 1713 coniferous forests, 1590 broadleaved forests and 1402 'mixed' forests) across Europe, comparing measured values from the LUCAS database (Toth *et al.*, 2013) to simulated steady-state estimates from the MEMS v1.0 model. All land uses are grouped for averages. Residuals are averaged across all sites within each NUTS2 region (populations between 800,000 and 3 million) and coloured accordingly. Measured site C stocks were subtracted from modelled values, meaning the model underestimates SOC stocks in positive (blue) regions and overestimates SOC stocks in negative (red) regions. Residuals average to within 10 Mg C ha^{-1} in areas with the lightest yellow colour. The size of circles within each region represents the number of sites simulated. Grey regions included no sites.

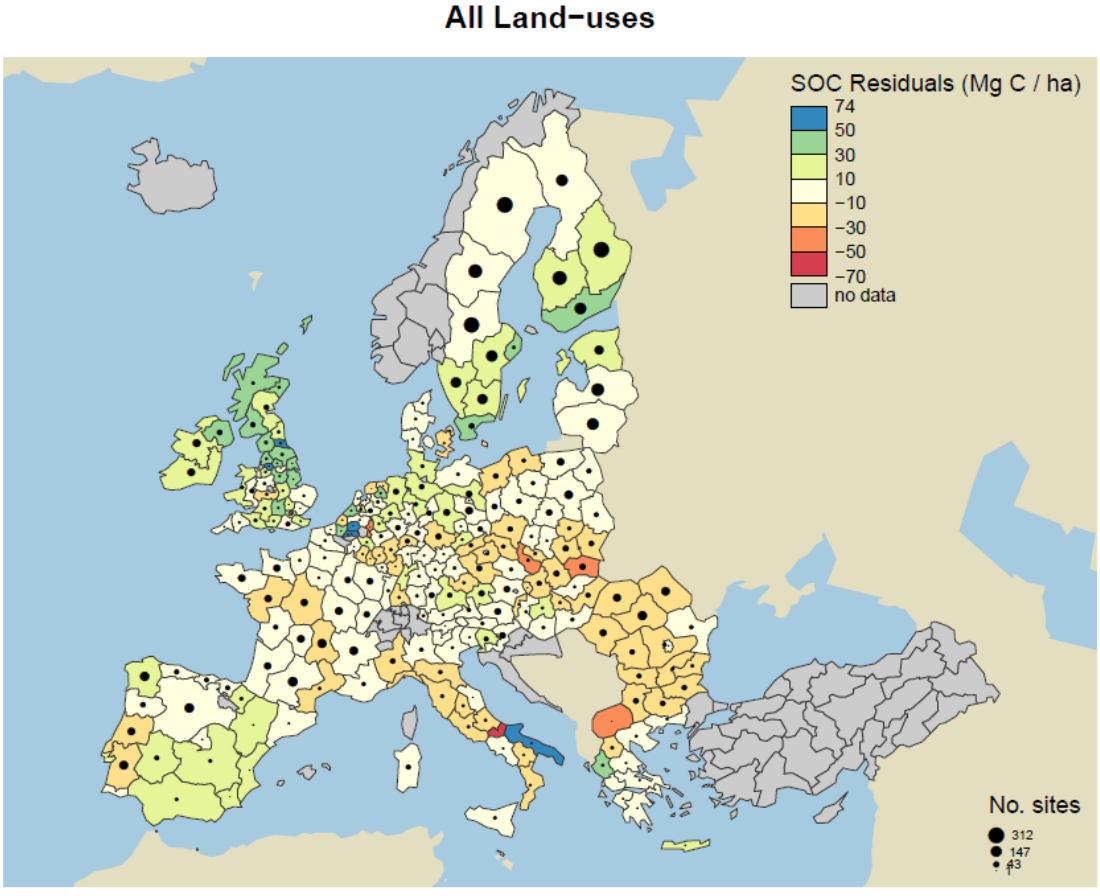

1030 **Tables**

1031 **Table 1 - State variables of MEMS v1.0 and fractionation definitions (measurement proxy and protocol) for isolating each**
1032 **pool. C1 to C4, and C6, refer to the litter layer, while C5 and C8 to C10 refer to the mineral soil. POM, Particulate organic**
1033 **matter; DOM, Dissolved organic matter; OM, Organic Matter. All SOM fractions are primary fractions obtained after**
1034 **dispersion to break up aggregates. For detail on a fractionation scheme to quantify each pool of the MEMS model please**
1035 **refer Table S1.**

1036

State variable	Pool description	Measurement proxy	Method reference
C1	Water soluble litter	Hot-water extractable C	Tappi (1981)
C2	Acid-soluble litter	Hydrolyzable fraction	Van Soest and Wine (1968); Van
C3	Acid-insoluble litter	Unhydrolyzable fraction	Soest *et al*. (1991)
C4	Microbial biomass	Direct extraction	Various (e.g., Setia *et al*., 2012)
C5	Coarse, heavy POM	> 1.8 g cm^{-3} and > 53 µm C	Christensen, 1992
C6	Litter layer DOM	< 0.45 µm extractable C	Kolka *et al*., 2008
C7	Emitted CO_2	Heterotrophic soil respiration	See Subke *et al*., 2006
C8	Soil layer DOM	< 0.45 µm extractable C	Kolka *et al*., 2008
C9	Mineral-associated OM	> 1.8 g cm^{-3} and < 53 µm C	Christensen, 1992
C10	Light POM	< 1.8 g cm^{-3}	Christensen, 1992
C11	Leached DOM	Suction cups / pans etc.	See Kindler *et al*., 2011

1037
1038

1039

Biogeosciences Discuss., https://doi.org/10.5194/bg-2018-430
Manuscript under review for journal Biogeosciences
Discussion started: 17 October 2018

1040 **Table 2 - Description and default values of all parameters used with MEMS v1.0. Where possible, notation has been used**
1041 **to remain consistent with further details in the supplementary information. Driving variables are reported in Table 3.**
1042 **Ranges are indicative of those observed in literature. Refer to Materials and Methods and Table S2 for details of the**
1043 **optimized parameter ranges.**

1044

Parameter	Parameter definition	Default value (range)	Units	Reference(s)
$B1$	Maximum growth efficiency of microbial use of water-soluble litter carbon (C1)	0.6 (0.4 – 0.7)	g microbial biomass C/g decayed	Sinsabaugh *et al*., 2013
$B2$	Maximum growth efficiency of microbial use of acid-soluble structural litter carbon (C2)	0.5 (0.3 – 0.6)	g microbial biomass C/g decayed	Sinsabaugh *et al*., 2013
$B3$	Heavy, coarse particulate organic matter (C5) generation from microbial biomass carbon (C4) decay	0.33 (0.028 – 0.79)	g microbial products C/g decayed C	Campbell *et al*., 2016
LIT_{frg}	Carbon in structural litter inputs (C2 and C3) transported to soil particulate organic matter (C5 and C10) each time step	0.006 ($1{\cdot}10^{-5}$ – $2{\cdot}10^{-3}$)	g C/g C decayed	-
POM_{split}	Fraction of fragmented litter inputs that form heavy particulate organic matter (C5)	0.30 (0.07 – 0.83)	0-1 scaling	Poeplau and Don, 2013; Soong *et al*., 2016
DOC_{frg}	Carbon in litter layer DOM (C6) transported to soil DOM (C8) each time step	0.8 (0.2 – 0.99)	g DOM-C/g DOM-C	-
DOC_{lch}	Maximum specific rate of leaching to represent vertical transport of carbon in DOM through the soil profile	0.00438 ($1{\cdot}10^{-5}$ – 0.02)	g C day^{-1}	Trumbore *et al*. 1992
EH_{max}	Maximum amount of carbon leached from decayed acid-soluble litter carbon (C2) to litter layer DOM (C6)	0.15	g DOM-C/g decayed C	Campbell *et al*., 2016
EH_{min}	Minimum amount of carbon leached from decayed acid-soluble litter carbon (C2) to litter layer DOM (C6)	0.005	g DOM-C/g decayed C	Campbell *et al*., 2016
ES_{max}	Maximum amount of carbon leached from decayed water-soluble litter carbon (C1) to litter layer DOM (C6)	0.15	g DOM-C g decayed C^{-1}	Campbell *et al*., 2016
ES_{min}	Minimum amount of carbon leached from decayed water-soluble litter carbon (C1) to litter layer DOM (C6)	0.005	g DOM-C g decayed C^{-1}	Campbell *et al*., 2016
k_1	Maximum decay rate of water-soluble litter carbon (C1)	0.37 (0.16 – 0.70)	g C day^{-1}	Campbell *et al*., 2016
k_2	Maximum decay rate of acid-soluble litter carbon (C2)	0.009 (0.0011–0.0200)	g C day^{-1}	Campbell *et al*., 2016
k_3 *	Maximum decay rate of acid-insoluble litter carbon (C3)	0.0002 ($2{\cdot}10^{-5}$– $1{\cdot}10^{-3}$)	g C day^{-1}	Moorhead *et al*., 2013
k_4	Maximum decay rate of microbial biomass carbon (C4)	0.57 (0.11-0.97)	g C day^{-1}	Campbell *et al*., 2016
k_5	Maximum decay rate of heavy, coarse particulate soil organic matter (C5)	0.0005 ($6{\cdot}10^{-5}$– $1{\cdot}10^{-3}$)	g C day^{-1}	Campbell *et al*., 2016; Del Galdo *et al*., 2003
k_8	Maximum decay rate of soil DOM (C8)	0.00144	g C day^{-1}	Kalbitz *et al*., 2005
k_9	Maximum decay rate of mineral-associated soil organic matter (C9)	$2.2{\cdot}10^{-5}$ ($1{\cdot}10^{-5}$– $4{\cdot}10^{-5}$)	g C day^{-1}	Del Galdo *et al*., 2003
k_{10}	Maximum decay rate of light particulate soil organic matter (C10)	$2.96{\cdot}10^{-4}$ ($4{\cdot}10^{-3}$–$1{\cdot}10^{-4}$)	g C day^{-1}	Del Galdo *et al*., 2003

la_2	Carbon leached from decayed microbial biomass carbon (C4)	0.19 (0.022 – 0.42)	g DOM-C g decayed C^{-1}	Campbell *et al*., 2016
la_3	Carbon leached from acid-insoluble litter carbon and heavy, coarse particulate organic matter carbon (C3 and C5)	0.038 (0.014 – 0.050)	g DOM-C g decayed C^{-1}	Campbell *et al*., 2016; Soong *et al*., 2015
LCI_{max}	Maximum lignocellulosic index that influences DOM generation from litter decay	0.51	-	Campbell *et al*., 2016; Soong *et al*., 2015
N_{max}	Maximum N content that influences rates (above this, there is no limit) of DOM generation and microbial carbon assimilation	3	%	Sinsabaugh *et al*., 2013
N_{mid}	Mid-point of logistic function that describes N limitation	1.75	%	Campbell *et al*., 2016; Soong *et al*., 2015
T_{opt}	Optimum temperature at which decay rates are highest	45	°C	Harmon and Domingo, 2001
T_{Q10}	Rate at which the decomposition rate increases with a 10 °C increase in soil temperature	2	-	Harmon and Domingo, 2001
T_{ref}	The reference temperature of estimated maximum decay rates (i.e., parameters k_x)	13.5	°C	Del Galdo *et al*., 2003
T_{shp}	Shape of the excessive temperature limitation for temperature modifier on decay rates beyond optimum temperature	15	-	Harmon and Domingo, 2001
T_{lag}	Difference from optimum temperature to the decline above that threshold applying to the temperature modifier on decay rates	4	°C	Harmon and Domingo, 2001
T_{range}	Difference between the maximum and minimum soil temperature values over a given year (*unused when temperature inputs are available*)	24	°C	Toth *et al*., 2013
SC_{icept}	Intercept coefficient used for the linear regression that estimates the maximum sorption capacity (parameter Q_{max}) of a soil	11.08	g C in < 53 µm fraction kg $soil^{-1}$	Six *et al*., 2002
SC_{slope}	Slope coefficient used for the linear regression that estimates the maximum sorption capacity (parameter Q_{max}) of a soil	0.2613	-	Six *et al*., 2002
${}^{L}k_{lm}$ *	Binding affinity for carbon in soil DOM (C8) sorption to mineral surfaces (C9) of the soil layer *L*	0.25	gC day^{-1}	Mayes *et al*., 2012; Abramoff *et al*., 2017
${}^{L}Q_{max}$ *	Maximum sorption capacity of mineral-associated soil organic matter carbon (C9) of soil layer *L*	-	gC m^{-2} $depth^{-1}$	Six *et al*., 2002

* These parameters are calculated as functions of others. For example, Q_{max} is a function of sand content, soil bulk density, rock fraction, SC_{icept} and SC_{slope}. More details can be found in the supplementary materials.

Biogeosciences Discuss., https://doi.org/10.5194/bg-2018-430
Manuscript under review for journal Biogeosciences
Discussion started: 17 October 2018

Table 3 - List of required driving variables for the MEMS v1.0 model. Baseline values represent mean values as reported in the LUCAS database (Toth *et al.*, 2013) of 8192 forest and grassland sites across Europe and were used for all qualitative testing and sensitivity analyses.

Driving variable	Symbol	Units	Baseline value	Land-use specific values				Reference
				Grassland	Broadleaf forest	Mixed forest	Coniferous forest	
Site condition variables								
Annual net primary productivity	*annNPP*	g C m^{-2} yr^{-1}	681	Site-specific values required				ORNL DAAC, 2009
Sand content of soil layer	*Sand*	%	47.8					Toth *et al.*, 2013
Bulk density of soil layer	*BD*	g cm^{-3}	1.21					
Rock fraction of soil layer	*Rock*	%	7.62					
Soil pH of layer	*pH*	-	5.58					
* Daily total carbon input	*CT*	g C m^{-2} day^{-1}	1.30					-
* Mean daily soil temperature	*soilT*	ºC	8.28					NOAA, 2018
Litter chemistry variables								
Hot-water extractable fraction	*fSOL*	0-1	0.45	0.35	0.40	0.38	0.35	Campbell *et al.*, 2016
Acid-insoluble fraction	*fLIG*	0-1	0.20	0.15	0.27	0.30	0.32	
Internal nitrogen content	*LitN*	%	1.00	1.10	1.32	0.87	0.41	
Root distribution variables								
Maximum rooting depth	*Rdepmx*	cm	300	260	290	340	390	Canadell *et al.*, 1996
Depth to which 50% of root mass is distributed	*Rdep50*	cm	20	15	25	27.5	30	Jackson *et al.*, 1996
Root to shoot ratio	*RtoS*	-	1.00	3.70	0.23	0.21	0.18	Jackson *et al.*, 1996

* - When daily measurements are not available annual values can be used to interpolate daily estimates. For more information please refer to the supplementary materials.

Biogeosciences Discuss., https://doi.org/10.5194/bg-2018-430
Manuscript under review for journal Biogeosciences
Discussion started: 17 October 2018

Table 4 - Evaluation results of comparisons between measured and modelled topsoil (0-20 cm) C stock for 8192 grassland and forest sites across Europe (see Figure 7 for geographic distribution of residuals). Mean absolute error (MAE) and mean bias error (MBE) describe the overall difference and directional difference between measured and modelled values, respectively. The model is deemed to describe the trend of the measured data better than the mean of the measurements when the modelling efficiency (EF) is positive, or when the Coefficient of Determination (CofD) is above 1. Each is a discrete evaluation metric. Divisions of high/low site conditions (mean annual temperature, mean annual precipitation, annual C inputs, sand content) were used to derive statistical significance (root mean square error, RMSE, and *F*-statistic) of differences between measured and modelled values while accounting for measurement variance within these divisions. An RMSE value below $RMSE_{95}$ indicates that simulated C stocks fall within the 95 % confidence interval of the measurements. An F-statistic below 0.05 also shows that simulated values are not significantly different to measurements at a 95 % confidence level.

		Evaluation metrics for individual site performance						Evaluation metrics using site condition *divisions* to include variance		
Land use	*n*	Mean ± 1 S.E. (Mg C ha^{-1})		MAE (Mg C ha^{-1})	MBE (Mg C ha^{-1})	EF	CofD	RMSE (Mg C ha^{-1})	$RMSE_{95}$ (Mg C ha^{-1})	*F*-statistic
		Observed	Predicted							
Pure grass	3487	65.9 ± 0.5	66.3 ± 0.3	24.7	-0.4	-0.047	4.52	13.0	10.3	0.009
Broadleaved	1590	71.2 ± 1.0	73.8 ± 0.4	31.0	-2.5	-0.062	5.54	19.0	14.7	0.052
Mixed Forest	1402	82.3 ± 1.1	75.2 ± 0.3	35.4	7.0	-0.173	8.36	12.9	19.2	0.042
Coniferous	1713	79.0 ± 1.1	76.3 ± 0.3	36.1	2.7	-0.057	10.35	13.5	18.7	0.006
* All	8192	72.5 ± 0.4	71.4 ± 0.2	30.2	1.1	-0.048	6.32	14.9	15.7	0.020

* All sites use 64 divisions (high/low site conditions and land use type)